Thermo-responsive Copolymers with Enzyme-dependent Lower Critical Solution Temperatures for Endovascular Embolization

by

Karime Jocelyn Rosas Gómez

A Thesis Presented in Partial Fulfillment
of the Requirements for the Degree
Master of Science

Approved April 2019 by the
Graduate Supervisory Committee:

Brent Vernon, Chair
Jessica Weaver
Amrita Pal

ARIZONA STATE UNIVERSITY

May 2019

ABSTRACT

Minimally invasive endovascular embolization procedures decrease surgery time, speed up recovery, and provide the possibility for more comprehensive treatment of aneurysms, arteriovenous malformations (AVMs), and hypervascular tumors. Liquid embolic agents (LEAs) are preferred over mechanical embolic agents, such as coils, because they achieve homogeneous filling of aneurysms and more complex angioarchitectures. The gold standard of commercially available LEAs is dissolved in dimethyl sulfoxide (DMSO), which has been associated with vasospasm and angiotoxicity. The aim of this study was to investigate amino acid substitution in an enzyme-degradable side group of an N-isopropylacrylamide (NIPAAm) copolymer for the development of a LEA that would be delivered in water and degrade at the rate that tissue is regenerated. NIPAAm copolymers have a lower critical solution temperature (LCST) due to their amphiphilic nature. This property enables them to be delivered as liquids through a microcatheter below their LCST and to solidify *in situ* above the LCST, which would result in the successful selective occlusion of blood vessels. Therefore, in this work, a series of poly(NIPAAm-*co*-peptide) copolymers with hydrophobic side groups containing the Ala-Pro-Gly-Leu collagenase substrate peptide sequence were synthesized as *in situ* forming, injectable copolymers.. The Gly-Leu peptide bond in these polypeptides is cleaved by collagenase, converting the side group into the more hydrophilic Gly-Ala-Pro-Gly-COOH (GAPG-COOH), thus increasing the LCST of the hydrogel after enzyme degradation. Enzyme degradation property and moderate mechanical stability convinces the use of these copolymers as liquid embolic agents.

DEDICATION

To my beloved parents, María Esther Gómez Martell and Gustavo Rosas Ruiz.

To the angels watching over me, Lorena Rosas, Gustavo Adán, and Pachis.

To my home country, México.

ACKNOWLEDGMENTS

First, I would like to thank my PI, Dr. Brent Vernon. I was very lucky to be in his Applied Learning Lab and subsequently join his research lab. I am very grateful for the valuable guidance and support he has given me and for introducing me to the endless possibilities of NIPAAm-based copolymers and Michael-addition reactions. Even with his busy schedule he made sure I was getting everything I needed in order to succeed and taught me what a great mentor is by being a great role model. I would also like to thank Dr. Amrita Pal; without her training, mentorship, patience and guidance, this work would have been much harder to complete. I greatly appreciate Dr. Vernon and Dr. Pal letting me be involved in other projects during my time in the lab. In addition, I would also like to thank Dr. Weaver for her valued input as part of my thesis committee. She supported the significance of this work and provided very insightful comments and recommendations for future work.

I would also like to acknowledge the undergraduate and high school students that I had the opportunity to mentor and train, including Karolena, Tori, Jay, Priscilla, Arianna, Michelle, Michael and Mahoro. Special thanks to Karolena Lein and Tori Johnson, who helped me with my experiments. I was very lucky to mentor you all throughout this work. In addition, I would also like to thank Dr. Heffernan and Dr. Overstreet, who I learned so much from.

Last but not least, I am very grateful to my family. Being away from home has not been easy, especially through the hard times we have had in the last few years. However, it is great to always have their love and support to fall back into. I especially would like to thank my parents, who have showed me true unconditional love and who have brought me

food from Mexico every time they come visit. Being raised by military parents gave me the discipline necessary to pursue a graduate degree and I could not be more thankful for that. I love you all very much.

TABLE OF CONTENTS

Page

LIST OF TABLES viii

LIST OF FIGURES ix

LIST OF ABBREVIATIONS xi

CHAPTER

1 INTRODUCTION AND BACKGROUND 1

1.1. A Brief History of Endovascular Embolization 1

1.2. Overview of Liquid Embolic Agents 2

1.3. Clinical Applications of Liquid Embolic Agents 3

1.3.1. High-flow Vascular Malformations 3

1.3.2. Aneurysms 5

1.3.3. Hypervascular Tumors 6

1.4 Commercially Available Liquid Embolic Agents 7

1.4.1. N-Butyl Cyanoacrylate (NBCA) 7

1.4.2. Onyx® 7

1.4.3. PHIL™ 10

1.5. Drawbacks of Liquid Embolic Agents 12

1.6. Introduction to N-isopropylacrylamide Polymers 13

1.7. Objective of the Thesis 15

CHAPTER Page

2 THERMO-RESPONSIVE COPOLYMERS WITH ENZYME-DEPENDENT LOWER-CRITICAL SOLUTION TEMPERATURES. 16

2.1. Introduction 16

2.2. Methods 17

2.2.1. Materials 17

2.2.2. Synthesis of Poly(NIPAAm-co-peptide) copolymers 18

2.2.3. ^{1}H Nuclear Magnetic Resonance 20

2.2.4. Enzyme Degradation 20

2.2.5. Cloud Point Determination 21

2.2.6. Rheology 22

2.3. Results 23

2.3.1. ^{1}H NMR 23

2.3.2. Cloud Point Determination 24

2.3.3. Rheology 30

2.4. Discussion 31

CHAPTER Page

3 CONCLUSION AND FUTURE WORK 36

3.1. Conclusion 36

3.2. Future Work 37

3.2.1. Optimization of Peptide Substitution 37

3.2.2. Incorporation of Cell-adhesive Peptides 37

3.2.3. Differential Scanning Calorimetry 38

3.2.4. Analysis of Thermo-responsive Gelation 38

3.2.5. Swelling Testing 39

3.2.6. Creep Resistance 40

REFERENCES 41

APPENDIX

A ^{1}H NMR Spectra of Synthesized Copolymers 50

LIST OF TABLES

Table Page

1. Polymer Composition, Storage Modulus (G'), Critical Strain and Cross-over Strain of Poly(NIPAAm-*co*-GAPGLX) Copolymers. 23
2. Half-max Absorbance LCST of Poly(NIPAAm-*co*-peptide) Copolymers. 26
3. Tangent Method LCST of Poly(NIPAAm-*co*-peptide) Copolymers. 26

LIST OF FIGURES

Figure Page

1. Chemical Structure Illustrating the Amphiphilic Nature pNIPAAm. Amide Groups Are Hydrophilic, and Isopropyl Groups Are Hydrophobic. 14
2. Chemical Structures of (A) GAPGLF-NH_2, (B) GAPGLL-NH_2, (C) GAPGLV-NH_2 and (D) GAPGLF-COOH. 17
3. Representation of LCST Determination by Half-max and Tangent Method from Turbidimetry. 21
4. ^{1}H NMR Spectra of pNIPAAm, Poly(NIPAAm-*co*-NASI), PNF-NH_2, and Poly(NIPAAm-co-GAPG-COOH). 24
5. Variation of LCST Depending on the Peptide Content in the Polymers Before Enzyme Degradation at 0.3 wt%. Relative Absorbance at 450 nm of PNV-NH_2 Copolymers with 0.1 mol% and 0.2 mol% in (A) HEPES and (B) PBS; PNF-COOH Copolymers with 0.2 mol% and 0.8 mol% in (C) HEPES and (D) PBS..... 27
6. Relative Absorbance at 450 nm Before and After Enzyme Degradation of (A) PNF-NH_2 at 0.3 wt% in HEPES and (B) PNF-NH_2 at 0.3 wt% in PBS, (C) PNL-NH_2 at 0.3 wt% in HEPES, and (D) PNV-NH_2 at 0.3 wt% in HEPES..... 28
7. Relative Absorbance at 450 nm of PNF-COOH with (A) 0.2 mol% and (B) 0.8 mol% Peptide Content Before and After Degradation at the Polymer Concentration of 0.3 wt% in HEPES. 29

Figure Page

8. Variation of LCST Due to Enzyme Degradation with Peptide Composition in (A) PNF-NH_2 by Half-max and Tangent Method, and (B) PNF-NH_2 and PNF-COOH by Tangent Method. 30
9. Storage Modulus (G') and Loss Modulus (G'') vs Applied Strain for (A) PNF-NH_2, (B) PNL-NH_2, (C) PNV-NH_2 Containing 0.1 mol% and (D) PNV-NH_2 Containing 0.2 mol% Peptide by Amplitude Sweep Under the Frequency of 1 Hz at the Polymer Concentration of 30 wt% in HEPES. 31
10. ^{1}H NMR Spectrum of PNF-NH_2. 51
11. ^{1}H NMR Spectrum of PNL-NH_2 51
12. ^{1}H NMR Spectrum of PNV-NH_2 with 4 mol% Peptide in Feed 52
13. ^{1}H NMR Spectrum of PNV-NH_2 with 8 mol% Peptide in Feed 52
14. ^{1}H NMR Spectrum of PNF-COOH with 2 mol% Peptide in Feed. 53
15. ^{1}H NMR Spectrum of PNF-COOH with 8 mol% Peptide in Feed. 53

LIST OF ABBREVIATIONS

Ala	Alanine
AVF	Arteriovenous Fistula
AVM	Arteriovenous Malformation
CT	Computerized tomography
dAVF	Dural Arteriovenous Fistula
DMSO	Dimethyl sulfoxide
EVOH	Poly(ethylene-vinyl alcohol)
FDA	Food and Drug Administration
Gly	Glycine
GRE	Gradient recalled-echo
^{1}H NMR	Proton nuclear magnetic resonance
HEPES	(4-(2-hydroxyethyl)-1-piperazineethanesulfonic acid)
LCST	Lower Critical Solution Temperature
LEA	Liquid embolic agent
Leu	Leucine
MW	Molecular weight
MWCO	Molecular weight cut off
NBCA	N-butyl cyanoacrylate
NIPAAm	N-isopropylacrylamide
PBS	Phosphate Buffered Saline
Phe	Phenylalanine

PHEMA	Poly(hydroxyethyl methacrylate)
PNF-COOH	Poly(NIPAAm-co-GAPGLF-COOH)
PNF-NH_2	Poly(NIPAAm-co-GAPGLF-NH_2)
pNIPAAm	Poly(N-isopropylacrylamide)
PNL-NH_2	Poly(NIPAAm-co-GAPGLL-NH_2)
PNV-NH_2	Poly(NIPAAm-co-GAPGLV-NH_2)
Pro	Proline
PVA	Poly(vinyl alcohol)
QT	Pentaerythritol tetrakis (3-mercaptopropionate)
SWI	Susceptibility-weighed imaging (SWI)
UV/Vis	Ultraviolet/Visible
Val	Valine

CHAPTER 1

INTRODUCTION AND BACKGROUND

1.1. A Brief History of Endovascular Embolization

Endovascular treatment decreases hospitalization time and speeds-up recovery as compared to open surgery.[1] The first reported embolization of head and neck cancers was made by Dawbarn with paraffin particles in 1904.[2] Later, Luessenhop and Spence performed the first reported cerebral arteriovascular malformation (AVM) embolization with silastic beads in 1960.[3] In 1971, Servinenko in Russia was the first to use detachable balloons.[4] The main disadvantage of detachable balloons, however, was that they deflated over time. The earliest CT scanner used to visualize the circulatory system as a tool to diagnose and treat blood vessel disease was first used for brain imaging in 1972.[5] Since then, advancements in technology have facilitated the minimally invasive delivery of liquid embolic agents. It was common procedure to puncture the surgically exposed carotid artery until Djindjan et al. in France in 1973 and Kricheff et al. in the USA in 1972 used the transfemoral route for catheter embolization.[6,7] Catheter-directed transarterial embolization was first reported in 1972 by Charles Dotter's group in the USA.[8] In 1975, Hilal and Michelsen used low-viscosity silicone polymer for the embolization of vascular tumors.[9] Cyanoacrylate glues that undergo polymerization in presence of blood were commercialized in the 1970s and have been used since then for the treatment of AVMs.[10] Cromwell and Kerber developed a balloon catheter that would enable the delivery of acrylic glue in a brain AVM without reflux and published his results in 1979.[11] Other embolic agents used in that time included Gelfoam®, silicone spheres, poly(vinyl alcohol) (PVA), and Ethibloc®.[12] Ethibloc®, no longer on the market, is a liquid embolic agent that

consists of a protein derived from maize and dissolved in Lipiodol® or additional alcohol, used predominantly for the embolization of vascular tumors and AVMs.[12] Coils for endovascular embolization were first introduced as small pieces of guidewire without the inner core, known as Gianturco coils, in 1975.[13] Later, more flexible platinum coils were developed; Guglielmi et al. introduced retrievable electrolytic detachable coils for cerebral aneurysms in 1991.[14] Currently, mechanical detachable coils are the gold standard for embolization procedures.[12]

1.2. Overview of Liquid Embolic Agents

The delivery of liquid embolics is done minimally invasively through a microcatheter that goes from the femoral artery into a feeding pedicle of an AVM, hypervascular tumor, or to the aneurysm site. Liquid embolics achieve homogeneous filling of aneurysms and more complex angioarchitectures present in vascular malformations and hypervascular tumors. Recanalization is also less common when using liquid embolics as compared to coils.[12] A shortcoming of embolic agents is the limited ability to penetrate the arterial vascular network as it increases in number of branches that gradually decrease in caliber, often resulting in incomplete embolization of AVMs.[15]

The distance traveled by liquid embolic agents depends on several factors, including viscosity, rate of injection, and microcatheter position.[16] Some liquid embolic agents are available in several concentrations with different viscosities. The lower viscosity formulations will travel more distally and penetrate deeper.[17] In some cases, it is appropriate to use a combination of different formulations for the same procedure. Embolization techniques include transvenous embolization with proximal balloon-protection, transarterial embolization and direct puncture. Precipitating liquid embolics

commercially available are typically dissolved in dimethyl sulfoxide (DMSO) or ethanol. Upon injection, the solvent dissipates with blood, causing the polymer to precipitate in situ into an embolus.[16,17]

1.3. Clinical Applications of Liquid Embolic Agents

1.3.1. High-flow Vascular Malformations

About 60,000 people have a high-flow vascular malformation in U.S. and around 240 will experience a hemorrhage, which presents a 15 to 20% risk of death or stroke and 30% neurological morbidity.[18] There are two types of vascular malformations that are treated by embolization: arteriovenous malformations, and arteriovenous fistulas.[19] Both types of vascular malformations present similar challenges in treatment. [19,20] Normally, blood flows from arteries to capillaries to veins. Capillaries serve to dampen blood pressure as it flows from arteries to veins. Arteriovenous malformations (AVMs) consist of feeding arteries, a network of small pathologic vessels in place of capillaries also referred to as the nidus, and draining veins.[21] AVMs often have several feeding arteries that supply blood to the nidus, also known as feeding pedicles that require embolization prior to resection.[22] Arteriovenous fistulas (AVFs) are abnormal connections between arteries and veins without the presence of a nidus or capillaries.[19] The absence of capillaries results in high-pressure blood flow into veins, which causes them to widen and often leads to rupture of the vessel wall. Cerebral AVMs may cause morbidity, neurological deficit and present a risk of hemorrhaging. [21] AVMs can be treated by transarterial embolization, transvenous embolization, direct puncture embolization, stereotactic radiosurgery, and surgical excision, alone or in combination. [15]

Surgical resection is recommended for the management of AVMs. Pre-surgical embolization is meant to ease surgical removal, decrease surgery complications and reduce blood loss during surgery. [12,23] The goal of endovascular embolization of AVMs is the closure of the whole nidus without occluding other surrounding vessels. [12,23] Successful penetration into the nidus and draining vein requires the microcatheter to be positioned less than 1cm from the nidus, which often cannot be achieved.[22] In such cases, occlusion of the arterial supply is sufficient if the AVM is surgically accessible for subsequent resection . [17,20,23] Incomplete resection or embolization may lead to further angiogenesis, which could increase the angioarchitecture complexity, thus making its subsequent treatment more challenging.[15] For example, angiogenesis may manifest as the creation of new feeders that may be too narrow to allow microcatheter access in subsequent treatment.[15]

A challenge that remains with AVFs when embolization is not accompanied by resection is that is that their high-flow nature has been reported to cause embolic materials to migrate into the distal draining veins, potentially resulting in unintentional pulmonary embolization.[15,20] Similarly, reflux of liquid embolics into the distal venous drainage or proximal arteries during embolization is often difficult to control and should be prevented. Surgical resection is necessary if venous drainage is observed.[15,24]

Some AVFs that have been reported to be treated successfully by endovascular embolization include dural, brain, and scalp arteriovenous fistulas. Dural arteriovenous fistulas (dAVFs) within the dura mater of the brain represent 10-15% of all intracranial AVMs.[17,25] They may present some disabling symptoms, and hemorrhage occurs in about 65% of patients.[25] Congenital brain arteriovenous fistulas account for 1.6 to 4.7% of all brain AVMs and are characterized by the absence of a nidus and their high-flow nature.[20]

Although they can be asymptomatic, they can also produce seizures, hemorrhage, increased intracranial pressure, among other symptoms that make treatment necessary.[20,21] The large draining vein can interfere with the exposure of the fistula making surgery challenging and not ideal. [20] Endovascular management facilitates localization of the lesion and enables access to deep and/or critical areas. [20] The heterogeneous angioarchitecture of scalp AVFs and non-uniform structure makes them challenging to treat.[15] Their high-flow shunting can lead to blood loss if the fistula is punctured during resection, for which endovascular management is generally recommended.[15]

1.3.2. Aneurysms

It is estimated that 6 million people in the United States have one or more unruptured brain aneurysms each year, 10% of which need treatment.[26] About 30,000 people in the U.S. suffer an aneurysm rupture each year, which can result in death in 40% of the cases, or permanent neurological deficit in 70% of those who survive.[26] The objective of treating aneurysms is their complete and permanent occlusion.[27] Ideally, this would be accompanied by the remodelling of the parent artery.

Saccular aneurysms are the most common type of intracranial aneurysm. They consist of a sac-like "dome" and a "neck" connected to one side of the parent artery wall or one of its main branches. LEAs achieve homogeneous and complete filling of aneurysms as opposed to coils. The use of platinum coils to treat large, wide-necked intracranial aneurysms often requires repeat treatment due to coil compaction as well as the use of a stent to prevent migration to nearby vessels.[27,28] Infectious aneurysms are also greatly benefitted from treatment with LEAs. Aneurysms with inflamed vascular tissue cannot be treated by surgical clipping due to the risk of clip erosion. Furthermore, infectious

aneurysms are often irregular in shape making endovascular embolization with LEAs ideal.[29]

The most common complication after endovascular aneurysm repair are type II endoleaks, characterized by the persistent perfusion within the aneurysmal sac and occur in 10 to 30% of patients.[16,30] Complex type II endoleaks may have a nidus as well as feeding and draining vessels.[30] Patients require follow-up CT imaging to assess the aneurysm sac size, size of the nidus, diameter of the feeding and draining vessels and the diameter of the feeding collateral artery to determine if intervention is necessary.[30]

1.3.3. Hypervascular Tumors

Presurgical endovascular embolization of hypervascular tumors has proven to mitigate blood loss, operative times and infection rates from surgical resection.[31,32] In addition, it may decrease surgical morbidity and mortality.[33] Some studies have pointed out the high associated cost of preoperative embolization of hypervascular tumors due to the large volume required for complete devascularization. [31] However, advantages of preoperative embolization, in addition to the low complication rate, have increased its preference.[31] For example, some physicians have reported that anterior skull based meningiomas fed by the ophthalmic artery benefit from embolization by reducing the risk of visual impairment.[33]

Usually devascularization is performed using polyvinyl alcohol (PVA) microparticles. [32] When the feeders to the metastatic region also supply the anterior spinal artery, which is the case for spinal hypervascular tumors, there is a risk that microparticles will migrate, posing a high risk of neurological complication.[32] When the vessels are small and tortuous, they may not be accessible by microcatheterization.[32] In such cases, direct puncture of the lesion is recommended to administer microparticles or LEAs if surgically

accessible.[32] Alternatively, injection of Onyx®, the leading liquid embolic agent, by endovascular route or by direct puncture has been used to successfully devascularize hypervascular tumors while providing a low risk of uncontrolled migration.[32]

1.4 Commercially Available Liquid Embolic Agents

1.4.1. N-Butyl Cyanoacrylate (NBCA)

NBCA (Trufill®, Cordis, Miami Lakes, Fl), also known as glue, is a nonabsorbable, adhesive embolic agent that polymerizes into a hard mass upon contact with ionic fluid and mixed with tantalum or tungsten powder for radioopacity.[12,15,25,29] It was approved by the FDA in 2000 for the treatment of brain AVMs.[34] It consists of 1 g tubes of NBCA, 10 mL of ethiodized oil, and 1 g of tantalum powder, all mixed before use.[35] Due to its rapid polymerization, it is necessary to rinse the microcatheter with a nonionic solution, such as a dextrose solution, prior to delivery to prevent microcatheter occlusion. [12,29] Rapid injection should be avoided because it could lead to retrograde embolization that could lead to microcatheter entrapment.[12] Ethiodized oil, such as Lipiodol, has been used to control the rate of polymerization.[12] However, even at high lipiodol dilution, it is unable penetrate the small feeding pedicles in an AVM before turning into a hard mass.[15] Another disadvantage of NBCA is its lack of biocompatibility, thus causing a significant vascular inflammatory reaction that can lead to angionecrosis. [15,36,37] Furthermore, it presents a high risk of recanalization; the largest study for dAVFs embolized with NBCA showed that only 33% of patients had complete occlusion at the 3-month postprocedure visit.[12,17]

1.4.2. Onyx®

Onyx® (Medtronic, Irvine, California) is a non-adhesive liquid embolic agent introduced in 1990 and approved by the FDA for endovascular treatment of AVMs in 2005 and the

leading LEA in the market.[21,24,25,38] It is composed of 67 mol% polyethylene (PE) and 33 mol% polyvinyl alcohol (PVA), commonly referred to as ethylene-vinyl alcohol (EVOH), and micronized tantalum for radioopacity dissolved in dimethyl-sulfoxide (DMSO).[1,12,23,25,39] PE is hydrophobic and PVA is hydrophilic, so Onyx® has both properties, which contribute to its cohesiveness.[24] Onyx ®18, 20, 34 and Onyx®-HD 500 (numbers indicating viscosity in centistokes) contain 6%, 6.5%, 8%, and 20% EVOH, respectively.[21,27,30,40] Onyx® HD-500+ contains 20% EVOH, but with higher tantalum concentration.[27] It is supplied as two 1.5 mL glass vials, one containing EVOH plus tantalum and the other one containing DMSO.[41]

All formulations require shaking for at least 20 minutes before injection to achieve a homogeneous solution.[21,23] Prior to delivering EVOH, 2 ml of DMSO are injected to irrigate the catheter lumen in order to prevent the copolymer from solidifying before reaching the embolization site.[24] The polymer precipitates in situ when it contacts blood as the solvent diffuses from the mixture and solidifies completely over a period of about 10 minutes, resulting in a pliable, rubbery, spongy, compressible material.[1,12,15,23,30,31,39] Complete filling with Onyx® is achievable, but antiplatelet therapy is necessary due to the risk of having small portions of the material pass into the parent artery. [27,40]

Onyx® 18, 20, and 34 are approved for the presurgical embolization of intracranial AVMs. [40] Onyx® 18 is often used in combination with Onyx® 34 for the treatment of AVMs, AVFs and type II endoleaks.[15,30] Successful treatment of dAVFs has been reported extensively in literature with up to 80% complete occlusion rate at the 3-month post-procedure follow-up.[17,25,42] Onyx® has also been used in combination with coils in the treatment of AVFs.[20] Detachable coils provide a template for Onyx® deposition, create

turbulent flow that promotes diffusion, and provide a physical barrier that minimizes the risk of distal embolization.[20] Onyx® 18 and 34 have also been administered off-label with good results by endovascular route for the embolization of spinal hemangioma, juvenile nasopharyngeal angiofibromas, paragangliomas and meningiomas, among other head and neck tumors.[32,43] In addition, it has produced satisfactory results by direct puncture for several skull base, head and neck tumors.[32]

Onyx® HD-500, designed to fill large or giant aneurysms, is FDA approved for the treatment of broad-base, sidewall, intracranial aneurysms.[27,40] Onyx® HD-500 has also been used for the immediate and complete occlusion a large ruptured intracranial pseudoaneurysm arising from a large, proximal intracranial artery, without the need for vessel sacrifice.[40] However, the treatment of unruptured saccular aneurysms with Onyx® is associated with up to 15.7% permanent morbidity and up to 4% mortality.[27] The mortality rate increases to over 20% for giant aneurysms.[27]

Advantages of Onyx® as compared to NBCA are its more permanent nature, low viscosity, non-adhesiveness and delayed precipitation, which allows for a slower, more deliberate delivery and better penetration.[21,30,31] Controlled administration, propagation, and gradual centripetal precipitation allows for a better chance to completely embolize the nidus as well as the feeding and draining vessels in AVMs.[1,30,31] A study showed that, due to its better penetration, the chance of not requiring surgical resection post-embolization was 81.8% with Onyx® versus 22.22% with NBCA.[44] However, although Onyx® 18 has a high ability to penetrate up to 5 micrometer diameter vessels, it is also more likely to reflux proximally from the microcatheter tip. [15,45] Excessive reflux along the catheter could lead

to unwanted occlusion of more proximal vessels.[39] In addition, catheter entrapment could occur if left in contact with the embolic agent for too long. [24,39]

There are also some issues associated with tantalum in Onyx®. Tantalum has a tendency to aggregate, which may result in microcatheter blockage.[39] It also poses a risk of sparking and combustion during subsequent surgical resection of AVMs when exposed to mono-polar diathermy, monopolar cautery, or high-energy bipolar cautery.[15,16,21,46] In addition, large amounts of Onyx® could result in dense radio-opaque saturation that decreases visibility.[23] Post-operative assessment is challenging because Onyx® produces significant streak artifacts on CT scans, gradient recalled-echo (GRE) and susceptibility-weighed imaging (SWI) sequences. [16,23,30] In addition, the dark color of tantalum limits its use for facial AVMs due to tattoo effect.[23]

There are also several disadvantages associated with DMSO. After successful procedures, some patients have reported nausea, headache and a strong garlic-like odor from their breath and/or sweat for 24 to 48 h caused by metabolism of DMSO.[30] DMSO may cause severe vasospasm that could lead to vasoconstriction if injected rapidly.[1,30,38,47] The acceptable injection rate for DMSO was found to be 0.2 mL/min, so the procedure takes from 1-3 h after preparation.[1,48]

1.4.3. PHIL™

PHIL™ (Microvention, Tustin, California) was approved by the FDA in 2016 for use in arteriovenous malformations and hypervascular tumors.[16,21] It is a non-adhesive liquid embolic agent comprised of a biocompatible copolymer, poly(lactide-co-glycolide) and poly(hydroxyethyl methacrylate) (PHEMA), covalently bonded to an iodine component for radio-opacity and dissolved in DMSO.[16,21,23,49,50] It is commercially available at

concentrations of 25, 30, and 35 wt%, with viscosities of 16, 36, and 72 cSt and embolic capacities of 0.85, 0.87, and 0.94 mL, respectively.[23] All compositions come in a pre-filled sterile syringe containing 1 mL of PHIL™ system that does not require prior preparation or shaking.[21] PHIL™ produces slower backflow, reducing the risk of unintended embolization of proximal vessels and has an aesthetic advantage over Onyx® for use in AVMs in the face due to its white color. [23] PHIL™ 35% has achieved complete occlusion of aneurysms and complete filling of dAVFs [17,49,50] Treatment of type II endoleaks has been performed successfully with different combinations of PHIL™ 25%, 30% and 35%.[16] However, PHIL™ 25% is more brittle and less pliable, so it could fragment and migrate to nearby vessels, which may give rise to several complications or death.[23]

The iodine radio-opaque agent, triiodophenol, is covalently bonded to the copolymer in PHIL™. Thus, there is no risk of radio-opaque agent aggregation or precipitation regardless of procedure time, resulting in a more homogenous fluoroscopic appearance and more consistent visibility as compared to Onyx®.[17,21,23] Iodine as radio-opacifier is also more advantageous during postinterventional imaging because it produces significantly less artifacts in CT scans and no artifacts in GRE and SWI.[17,21,23] However PHIL™ 25% has reduced visibility as compared to Onyx® 18 in small vessels because iodine is less radio-opaque.[17]

PHIL™ 25% has decreased injection times as compared to Onyx® because it precipitates faster, has a greater embolic capacity, and is benefitted from shorter pauses between injections.[17,21,23] PHIL™ 25% precipitates within 3 minutes, as compared to Onyx® 18, which takes 5 min to precipitate, resulting in faster plug formation and procedure time. [21,23] In addition, PHIL™ has greater embolic capacity at comparable

viscosities; 0.25 mL of PHIL™ 25 produces the same extent of embolization as 1 mL of Onyx® 18.[21] A study showed that shorter pauses between injections of PHIL™ 25% does not have adverse effects and results in better filling.[21] Better forward penetration has also been achieved with PHIL™; the smallest vessel reported to be occluded with PHIL™ 25% was 2.9 micrometers in diameter.[23]

Onyx® and PHIL™ are less thrombogenic than NBCA. [17] Thrombogenicity is desirable for complete occlusion with coils because it promotes the formation of a clot that fills the free space around coils.[51] However, it is not desirable on liquid embolics because they most often achieve more homogeneous occlusion. Thrombogenicity caused by LEAs would likely produce adverse effects.[51] Moderate vascular inflammation has been observed with LEAs dissolved in DMSO and accompanied by angionecrosis for Onyx®.[23]

1.5. Drawbacks of Liquid Embolic Agents

Reflux remains a major challenge among liquid embolic agents because it can be difficult to control. [12] Certain degree of reflux is desired for the formation of a polymeric cast "plug" around the catheter tip. [21,30]This enables deep penetration and improves antegrade movement of the embolic agent, while reducing the risk of excessive reflux. [21] However, excessive reflux is still common and can lead to embolization of non-target arteries and microcatheter entrapment.[21,39] In some cases, removal of entrapped microcatheters has resulted in intracranial hemorrhages.[39] Some techniques have been studied to reduce reflux and in turn reduce the likelihood of microcatheter entrapment. [39]

One approach is the simultaneous use of two microcatheters to deliver Onyx®; one microcatheter with a detachable tip was used to deliver Onyx®, while the other one was used to inject NBCA to glue the detachable tip to the precipitated Onyx®.[12,39] However,

this is not possible when the microcatheter cannot reach the feeding arteries.[12] The use of a dual-lumen balloon catheter is another way to minimize retrograde reflux that has showed clinical success for the treatment of brain aneurysms, AVMs and dAVFs with Onyx®.[12,25,37,39,52,53] For this approach, one lumen is used to inflate a balloon that prevents reflux, the second lumen delivers the liquid embolic agent.[39] However, due to their larger diameter, dual-lumen catheters are limited in use to higher caliber vasculature.[39] Moreover, balloon-assisted transvenous embolization may prevent reflux into proximal arteries, as opposed to embolization through the transarterial route which often produces excessive reflux.[15] However, the transvenous route is not always accessible.[15] An additional consideration with balloon catheters is that some may not be compatible with all liquid embolics, such as NBCA.[39,54]

1.6. Introduction to N-isopropylacrylamide Polymers

The thermal transition behavior of poly(N-isopropylacrylamide) (pNIPAAm) was first reported in 1967 by Scarpa et al.[55] pNIPAAm is a thermo-responsive polymer with a lower critical solution temperature (LCST) capable of undergoing a reversible phase transition or phase separation due to its amphiphilic nature, as shown in Figure 1. This property enables it to be soluble in aqueous solution below the LCST without the need of toxic solvents, and to solidify *in situ* if the LCST is below body temperature. Above the LCST, hydrogen bond activity from the amide groups decreases due to the breaking of hydrogen bonds between water and the NH and CO groups.[56] Consequently, hydrophobic interactions of isopropyl groups become dominant, resulting in a decrease in the solubility of the polymer, causing the polymer chains to collapse and precipitate if the concentration is sufficient.[56]

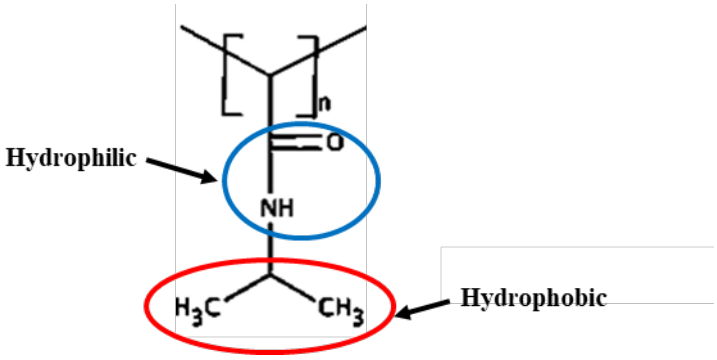

Figure 1. Chemical structure illustrating the amphiphilic nature pNIPAAm. Amide groups are hydrophilic, and isopropyl groups are hydrophobic.

The LCST of pNIPAAm can be modified by the addition of comonomers or side chains that affect its hydrophilicity. The use of hydrophilic comonomers has resulted in an increase of the LCST.[57] Similarly, the addition of hydrophobic comonomers is expected to decrease the LCST.[58] LCST can also vary according to the average molecular weight of the polymer, with lower molecular weights having lower LCST as compared to higher molecular weights.[59] In addition, higher buffer concentrations and higher pH have shown to decrease the LCST of pNIPAAm copolymers.[60] There are several methods of reporting LCST values for thermo-responsive polymers. Cloud point determination uses UV-Vis spectroscopy to examine the turbidimetry of a polymer solution at different temperatures and is the most popular method of measuring the LCST of a polymer.[61] It has been reported as the half-max absorbance value, the temperature corresponding to a 10% reduction in the transmittance of a solution, the temperature at the inflection point, as well as by the tangent method. [62] In addition, the temperature at which the first opaqueness is observed has previously been reported as the onset temperature and also as the LCST.[63] Cloud point determination takes advantage of changes in turbidimetry of the solution due to

hydrophobic interactions, which are faster in solutions with higher polymer concentration.[63]

1.7. Objective of the Thesis

The objective of this thesis was to synthesize a liquid embolic agent that is dissolved in non-toxic solvents and degrades at the rate that tissue is regenerated. A NIPAAm-based copolymer was chosen due to its ability to be injectable through a catheter in aqueous solution and precipitate *in situ*, eliminating the need for a toxic solvent. Hydrophobic peptides that become more hydrophilic upon degradation by collagenase were chosen as side groups. Therefore, as cells migrate and remodel the vessel wall, the LCST of the polymer would increase to above body temperature and subsequently redissolve into the bloodstream instead of fragmenting and migrating into nearby vessels. Furthermore, this work investigated different hydrophobic peptides to determine which one produced the greatest LCST change upon degradation and the greatest mechanical stability.

CHAPTER 2

THERMO-RESPONSIVE COPOLYMERS WITH ENZYME-DEPENDENT LOWER-CRITICAL SOLUTION TEMPERATURES.

2.1. Introduction

N-isopropylacrylamide (NIPAAm) copolymers have a lower critical solution temperature (LCST) due to their amphiphilic nature, which allows them to be injectable below LCST and to solidify *in situ* above the LCST, if the concentration is sufficient, and are widely used in biomedical applications. [57] To decrease chronic inflammatory response in controlled drug delivery applications, several hydrolyzable side groups have been used in those biodegradable NIPAAm-based copolymers. Recently, a number of NIPAAm based copolymers have been developed which respond to specific biological targets such as enzymes, resulting in the degradation of the copolymer-based hydrogel.[57,64,65] The aim of this study was to investigate amino acid substitution in an enzyme degradable side group of a NIPAAm copolymer for drug delivery and bioresorbable scaffolds for tissue engineering. Therefore, in this work, a series of NIPAAm-based copolymers with hydrophobic side groups containing the Ala-Pro-Gly-Leu collagenase substrate peptide sequence were synthesized as *in situ* forming, injectable copolymers. Collagenase is a matrix metalloproteinase (MMP) that plays an important role enabling cell migration and tissue remodelling. [64,66] The Gly-Leu peptide bond in these polypeptides is cleaved by collagenase, converting the side group into the more hydrophilic GAPG-COOH, thus increasing the LCST of the hydrogel. [57]The side groups Gly-Ala-Pro-Gly-Leu-Phe-NH_2 (GAPGLF-NH_2), Gly-Ala-Pro-Gly-Leu-Leu-NH_2 (GAPGLL-NH_2), Gly-Ala-Pro-Gly-Leu-Val-NH_2 (GAPGLV-NH_2), and Gly-Ala-Pro-Gly-Leu-Phe-COOH (GAPGLF-

COOH) were used to synthesize poly(NIPAAm-*co*-GAPGLF-NH_2) (PNF-NH_2), poly(NIPAAm-*co*-GAPGLL-NH_2) (PNL-NH_2), poly(NIPAAm-*co*-GAPGLV-NH_2) (PNV-NH_2), and poly(NIPAAm-*co*-GAPGLF-COOH) (PNF-COOH) copolymers.

2.2. Methods

2.2.1. Materials

N-isopropylacrylamide (NIPAAm, TCI chemicals) was purified by recrystallization in hexane, filtered, and vacuum dried for 3 days. 2,2'-Azobisisobutyronitrile (AIBN, Aldrich) was purified by recrystallization in methanol. GAPGLF-NH_2 (F-NH_2), GAPGLL-NH_2 (L-NH_2) and GAPGLV-NH_2 (V-NH_2) peptides were obtained from the Biodesign Institute (Tempe, AZ). GAPGLF-COOH (F-COOH), >95% purity, was purchased from Genscript. Structures of peptides are shown in Figure 2. N-acryloxysuccinimide (NASI), tetrahydrofuran (THF), triethylamine (TEA), and ethyl ether were obtained from Sigma Aldrich. 125mM HEPES and 150 mM PBS buffer solutions, pH 7.4, were used for cloud point measurements. 125mM HEPES + 5mM $CaCl_2$ buffer solution and 150mM PBS buffer solution + 5mM $CaCl_2$, pH 7.4, were prepared for use during enzyme degradation studies. Sigma blend type F collagenase from clostridium histolyticum was purchased from Sigma Aldrich.

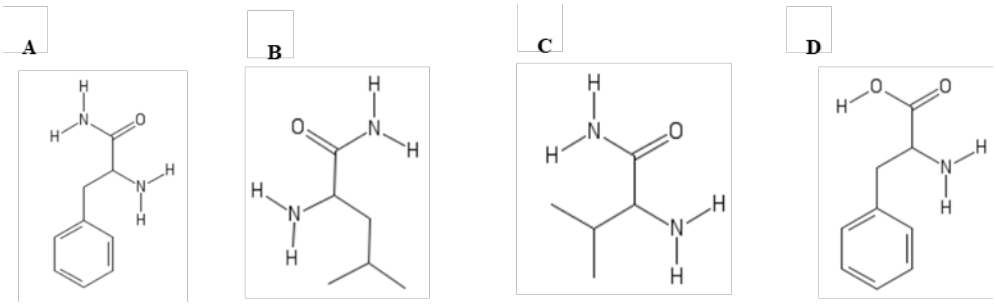

Figure 2. Chemical structures of (A) GAPGLF-NH_2, (B) GAPGLL-NH_2, (C) GAPGLV-NH_2 and (D) GAPGLF-COOH.

2.2.2. Synthesis of Poly(NIPAAm-co-peptide) copolymers

Poly(NIPAAm-*co*-peptide) copolymers and pNIPAAm were synthesized according to previous literature[57], as shown in Scheme 1. Poly(NIPAAm-*co*-NASI) was synthesized by reacting NIPAAm with NASI by free radical polymerization at a molar feed ratio of 90:10 in THF with AIBN as the initiator. The reaction was carried out under a nitrogen environment at 65ºC for 24 h. The product was precipitated in ethyl ether, vacuum dried, dialyzed (3.5 kDa MWCO) for 3 days at 4ºC and lyophilized before peptide substitution. Poly(NIPAAm-*co*-NASI) was used to synthesize pNIPAAm and poly(NIPAAm-*co*-peptide) copolymers. 50-fold N-isopropylamine, and TEA, equimolar with NASI, were added to a 10 wt% solution of poly(NIPAAm-*co*-NASI) in THF and allowed to react for 24 h to obtain pNIPAAm homopolymer. Peptide and triethylamine (TEA), equimolar with peptide, were added to a 10 wt% solution of poly(NIPAAm-*co*-NASI) in THF. The reaction was carried out under a nitrogen environment at 50ºC for 72 h. The remaining NASI groups were backreacted with 50-fold N-isopropylamine at 50ºC for 24 h to obtain poly(NIPAAm-*co*-peptide) polymers. The product was then filtered to removed succinimide salts, precipitated in cold ethyl ether, filtered to recover the product, vacuum dried, dialyzed (3.5 kDa MWCO) at 4ºC for 6 h and lyophilized.

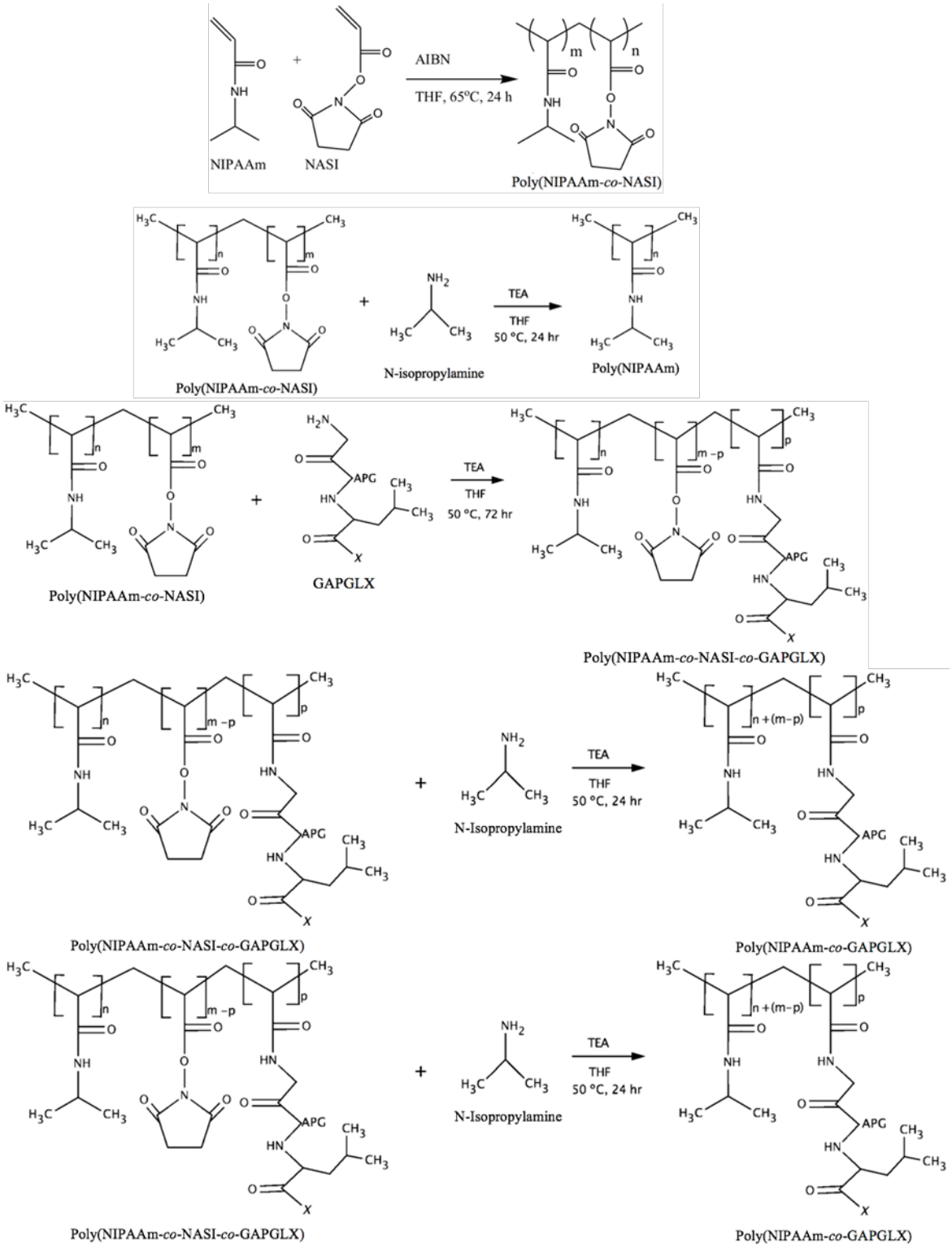

Scheme 1. Reaction synthetic scheme for pNIPAAm and poly(NIPAAm-*co*-GAPGLX), where X is F-NH_2, L-NH_2, V-NH_2, or F-COOH.

2.2.3. ^{1}H Nuclear Magnetic Resonance

^{1}H NMR measurements were made with a 400 MHz Bruker spectrometer using 10mg/750μL polymer solutions in a deuterated solvent. Deuterated chloroform ($CDCl_3$) and deuterium oxide (D_2O) were used as solvents. ^{1}H NMR was used to confirm the successful synthesis of poly(NIPAAm-*co*-NASI) and poly(NIPAAm-*co*-peptide).

2.2.4. Enzyme Degradation

5 wt% samples of poly(NIPAAm-*co*-peptide) were prepared in 125 mM HEPES or 150 mM PBS standard buffer solutions, pH 7.4, containing 5 mM $CaCl_2$ and kept at 25ºC. Collagenase solution was prepared fresh every day at 40 mg/mL concentration and 10µL of it was added per 1 mL of polymer solution every day for 5 days. Control samples were maintained without enzyme. After 5 days, solutions were dialyzed (3.5 kDa MWCO) at 4ºC for 3 h and lyophilized. Scheme 2 shows the enzyme degradation reaction scheme for poly(NIPAAm-*co*-peptide) copolymers.

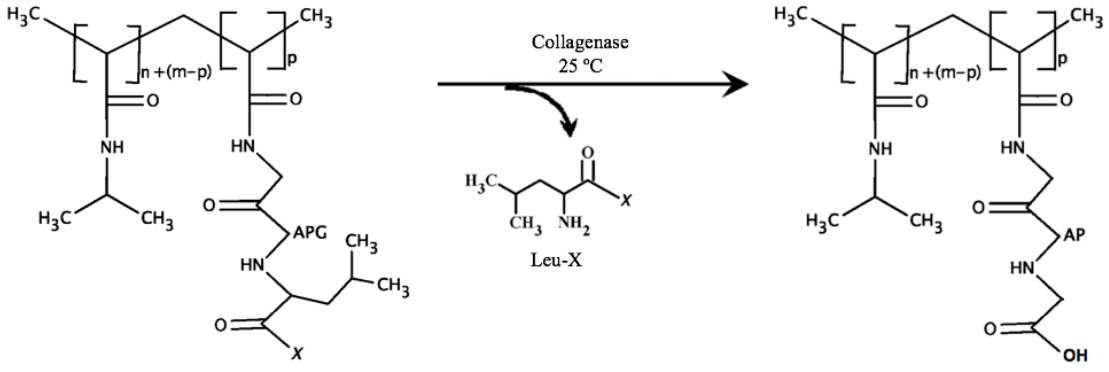

Scheme 2. Enzyme degradation by collagenase of poly(NIPAAm-*co*-GAPGLX), where X is F-NH_2, L-NH_2, V-NH_2, or F-COOH.

2.2.5. Cloud Point Determination

LCST before and after enzyme degradation was determined by cloud point measurement using UV spectrophotometer by half-max and tangent method, as shown in Figure 3. Polymer samples were dissolved at 0.3 wt% in buffer solution. Cuvettes containing the polymer solutions were heated in a water bath and the relative absorbance at 450 nm was measured from 20 ºC to 40 ºC every 1 ºC increase, and from 40ºC to 60 ºC every 5 ºC increase. Each measurement was taken every 5 minutes after increasing the temperature. 125 mM HEPES and 150 mM PBS standard buffer solutions, pH 7.4, were used for absorbance measurements. Cuvettes containing buffer alone were used as reference.

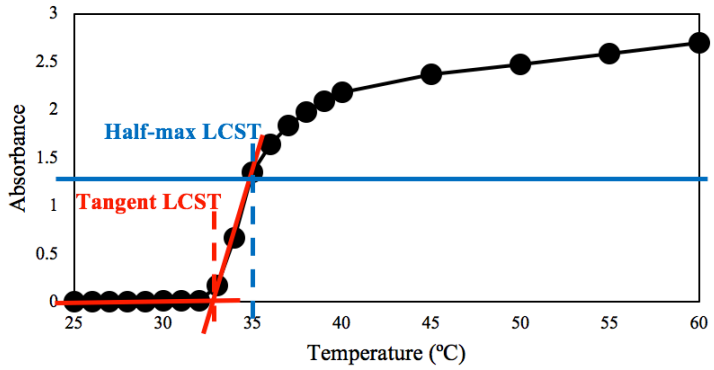

Figure 3. Representation of LCST determination by half-max and tangent method from turbidimetry.

Half-max Method

In some polymer solutions, the increase in temperature causes aggregation and subsequent precipitation. As a result, the absorbance reaches a maximum and then continues to decrease as temperature is further increased.[58] For other polymer solutions, the absorbance continues to increase as temperature is increased.[58] For both cases, the LCST is determined as the temperature at which the curve is at 50% maximum absorbance, as shown in Figure 3.[57,67]

Tangent Method

This method consists of fitting two lines on the relative absorbance vs temperature curve obtained by UV/Vis spectroscopy. One line corresponding to the baseline before any increase in relative absorbance, while the other line corresponds to the tangent at the inflection point of the curve. The tangent method LCST is the temperature at which the tangent line to the inflection point and the line on the baseline intercept each other, as shown in Figure 3. [68,69]

2.2.6. Rheology

Mechanical stability of the gel formed by 30 wt% polymer in 125 mM HEPES buffer solution (pH 7.4) was measured at 37 ºC using a Physica MCR 101 (Anton Paar) rheometer. Parallel plate geometry of 25 mm diameter and a 0.2 mm gap were used for the rheology measurements. Amplitude sweep was performed from 0.01 to 100% strain under the frequency of 1 Hz at 50 mN normal force. Storage moduli (G') were reported at 0.5% strain.

2.3. Results

2.3.1. ^{1}H NMR

^{1}H NMR was used to confirm the polymerization of NIPAAm monomer with NASI. NASI was added as a good leaving group to be substituted by the peptide or N-isopropylamine, both of which become partially negative due to the presence of TEA.[58] The mole ratio of NIPAAm and NASI was calculated from the integration ratio between the lone proton of the isopropyl group of NIPAAm [1H, $(CH_3)_2CHNHCO$], appearing at ~3.89 ppm, and the methylene protons of NASI [4H, $(CH_2)_2(CHO)_2NOCO$], appearing at ~2.89 ppm, as shown in **Error! Reference source not found.**. The NASI content in poly(NIPAAm-*co*-NASI) was determined to be 7.83 mol%. The mole ratios of NIPAAm and peptide on Table 1 were determined by the integration ratio between the lone proton of the isopropyl group of NIPAAm and the methyl protons of leucine [6H, GAPG($(CH_3)_2CHNHCO$)X], appearing between ~0.9 and 1 ppm, as seen in Figure 4. The disappearance or reduction in the peak corresponding to the methyl protons of leucine confirmed the cleavage of the Gly-Leu bond, as seen in **Error! Reference source not found.**. The values in Table 1 indicated that the peptide content in the synthesized polymers are much lower than actual feed. The ^{1}H NMR spectra of synthesized polymers are presented in Figure 10-15 in Appendix A.

Table 1. Polymer composition, storage modulus (G'), critical strain and cross-over strain of poly(NIPAAm-*co*-GAPGLX) copolymers.

	Peptide content[a]		*Storage Modulus*[b]	*Critical Strain*[b]	*Cross-over Strain*[b]
Polymer	*Feed*	*Composition*	*(kPa)*	*(%)*	*(%)*
PNF-NH_2	4%	6.10%[57]			
	4%	1.49%	71.9	0.6	3
PNL-NH_2	4%	0.19%	51.4	2	8
PNV-NH_2	4%	0.13%	12.9	2	7
	8%	0.23%	14.8	1	7
PNF-COOH	2%	0.22%			
	8%	0.76%			

[a]Peptide content is in mol%.
[b]Storage modulus (G') at 0.5% strain, critical strain (%) and cross-over strain (%) of poly(NIPAAm-co-GAPGLX) copolymers at 30 wt% in 125 mM HEPES buffer solution, 7.4 pH.

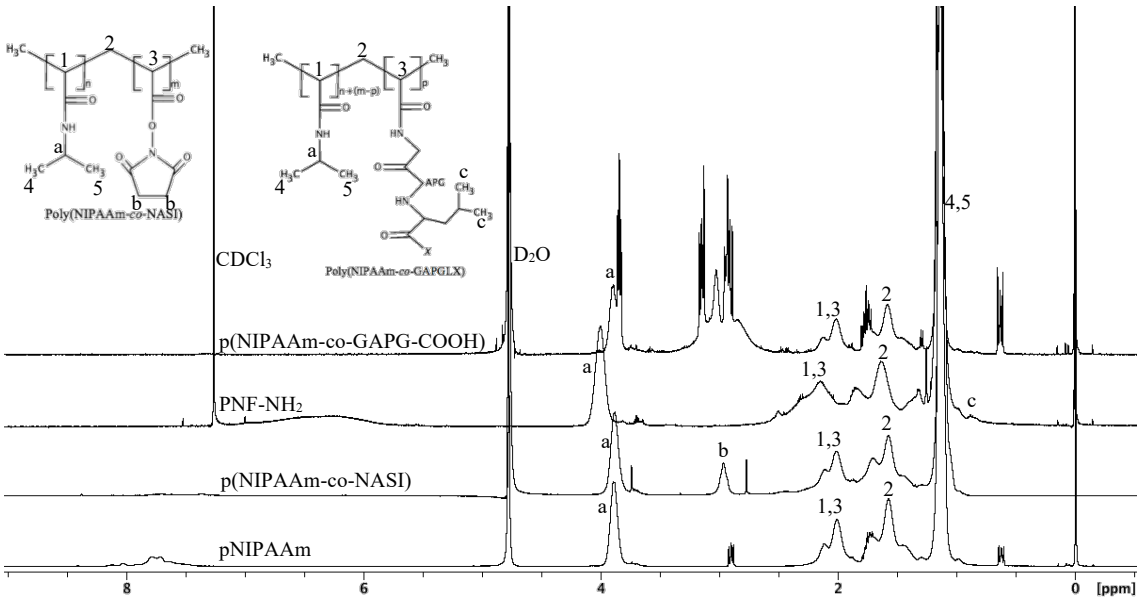

Figure 4. ^{1}H NMR spectra of pNIPAAm, poly(NIPAAm-*co*-NASI), PNF-NH_2, and poly(NIPAAm-co-GAPG-COOH).

2.3.2. Cloud Point Determination

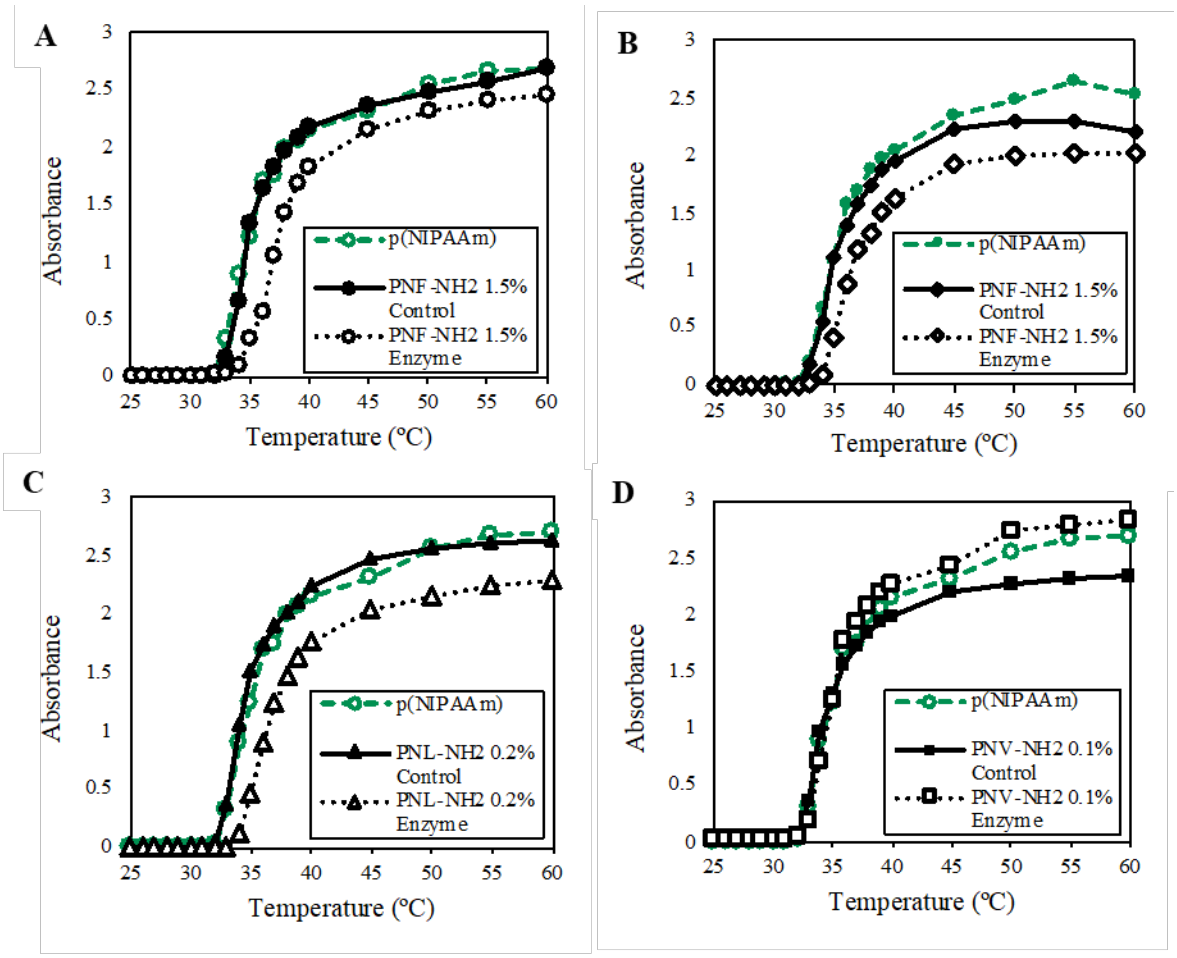

Figure 6-7 show the cloud point data for the copolymers synthesized. This data was used to determine the LCST of the copolymers. Enzyme degradation of PNF-NH_2, PNL-NH_2, PNV-NH_2 and PNF-COOH copolymers was carried out in HEPES containing 5mM $CaCl_2$. In addition, enzyme degradation for PNF-COOH copolymers was also done in PBS containing 5mM $CaCl_2$. LCST was determined by half-max absorbance temperature (Table 2) and tangent method (Table 3) before and after degradation.

It was observed that doubling the amount of peptide (from 0.13 to 0.23 mol%) for PNV-NH_2 increased the LCST by ~2 ºC (from 34.5 to 36.4 ºC) according to the half-max method (Table 2), and by ~1.5 ºC (from 32.0 to 33.4 ºC) as determined by the tangent

method (Table 3) (Figure 5). PNV-NH_2 containing 0.13 mol% peptide resulted in 0.6 ºC LCST change (from 34.5 to 35.3 ºC), after enzyme degradation, as determined by half-max method (**Error! Reference source not found.**), which is similar to the LCST change calculated to be 0.7 ºC (from 32.0 to 32.7 ºC) by tangent method (Table 3)(Figure 6). PNL containing 0.19 mol% peptide resulted in 2.1 ºC LCST change (from 34.6 to 36.7 ºC), determined by half-max method (

Table **2**), while the LCST change is 1.4 ºC (from 32.3 to 33.7 ºC) as calculated from tangent method (Table 3) (Figure 6). For PNF-NH_2 copolymers, 4-fold increase in the GAPGLF-NH_2 (~1.5 to 6.1 mol%) content in the copolymer results in 3.5-fold increase in the LCST change (from 2.5 to 8.6 ºC), according to the half-max method (

Table **2**), whereas it results in 6-fold increase in the LCST change (from 1.6 to 9.1 ºC) according to the tangent method (Table 3)(Figure 6). Similarly, for PNF-COOH copolymers, 4-fold increase in the peptide content of GAPGLF-COOH (~0.2 to 0.8 mol%) results in 6-fold increase in the LCST change (from 0.6 to 3.5 ºC), according to the half-max method (

Table **2**), whereas it results in 4-fold increase in the LCST change (from 0.4 to 1.6 ºC), according to the tangent method (Table 3) (Figure 7). Thus, it was observed that the change in LCST from the tangent method differed from the LCST change calculated from the half-max method for PNL-NH_2, PNF-NH_2, and PNF-COOH, but not for PNV-NH_2. It also appeared that LCST change was more pronounced for PNF-COOH than for PNF-NH_2, according to the tangent-method (Table 3), both following a linear correlation of the LCST change with peptide content, as seen in Figure 8. Thus, peptide content needed to produce the desired LCST change could be extrapolated from this graph.

Table 2. Half-max absorbance LCST of poly(NIPAAm-*co*-peptide) copolymers.

		LCST before degradation (ºC)		*LCST after degradation[a] (ºC)*		*Change (ºC)*	
Polymer	*Peptide content (mol%)*	*HEPES*	*PBS*	*HEPES*	*PBS*	*HEPES*	*PBS*
poly(NIPAAm)	0 [a,57]	33.3	-	33.3	-	0	-
	0	33.2	33.5	33.2	33.5	0	0
PNF-NH_2	6.10%[a,57]	30.7	-	39.3	-	8.6	-
	1.49%	35.0	35.2	37.5	36.4	2.5	1.2
PNL-NH_2	0.19%	34.6	34.6	36.7	-	2.1	-
PNV-NH_2	0.13%	34.5	34.8	35.3	-	0.6	-
	0.23%	36.4	36.6	-	-	-	-
PNF-COOH	0.22%	35.3	35.5	35.9	-	0.6	-
	0.76%	36.0	36.0	39.5	-	3.5	-

[a]Poly(NIPAAm) and PNF-NH_2 containing 6.1 mol% peptide data obtained from Overstreet et al.[57]

Table 3. Tangent method LCST of poly(NIPAAm-co-peptide) copolymers.

		LCST before degradation(ºC)		*LCST after degradation(ºC)*		*Change (ºC)*	
Polymer	*Peptide content (mol%)*	*HEPES*	*PBS*	*HEPES*	*PBS*	*HEPES*	*PBS*
poly(NIPAAm)	0 [a,57]	29.5	-	29.5	-	0	-
	0	32.2	32.6	32.2	32.6	0	0
PNF-NH_2[a]	6.10%[57]	25.3	-	34.4	-	9.1	-
	1.49%	32.8	32.7	34.4	33.8	1.6	1.1
PNL-NH_2	0.19%	32.3	32.0	33.7	-	1.4	-
PNV-NH_2	0.13%	32.0	32.5	32.7	-	0.7	-
	0.23%	33.4	34.0	-	-	-	-
PNF-COOH	0.22%	32.9	33.5	33.3	-	0.4	-
	0.76%	33.2	33.0	34.8	-	1.6	-

[a]poly(NIPAAm) and PNF-NH_2 containing 6.1 mol% peptide data obtained from Overstreet et al.[57]

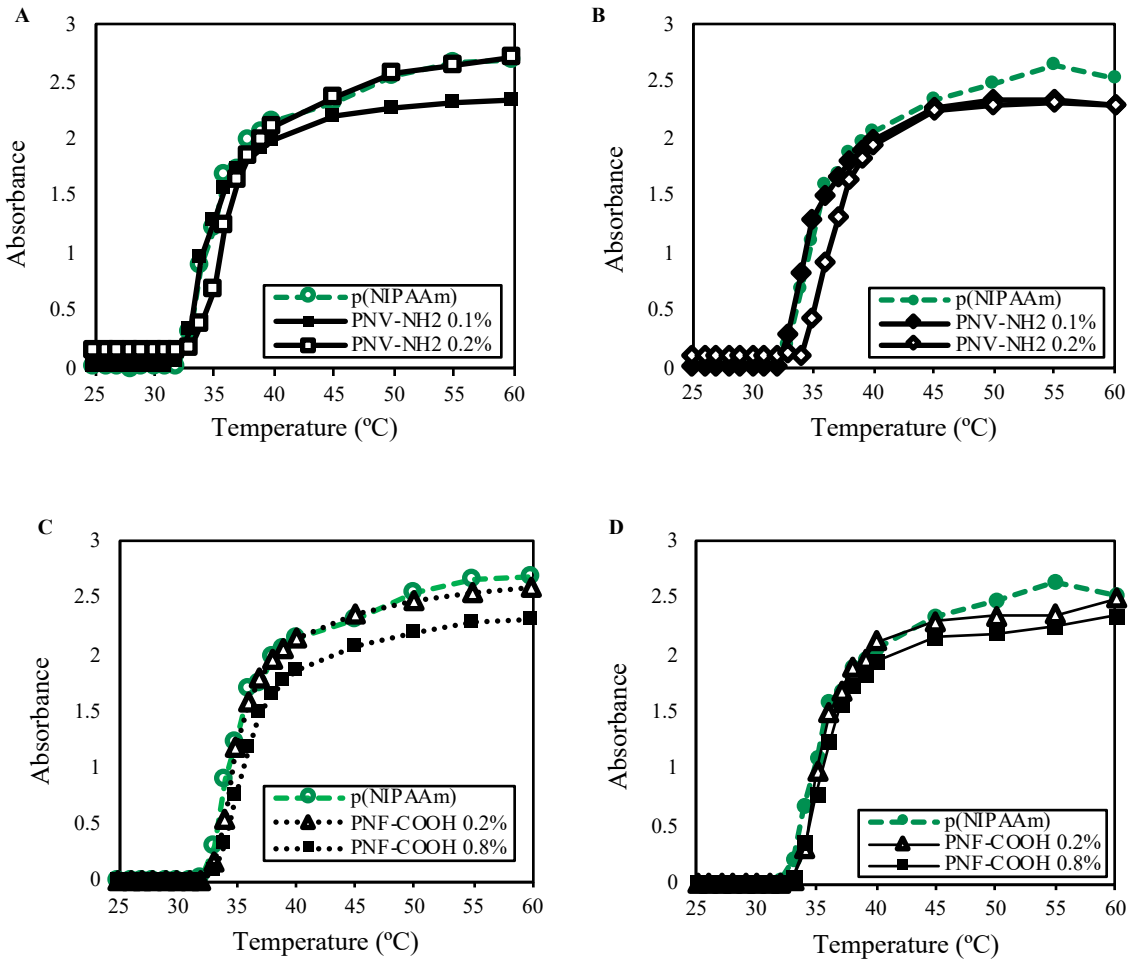

Figure 5. Variation of LCST depending on the peptide content in the polymers before enzyme degradation at 0.3 wt%. Relative absorbance at 450 nm of PNV-NH_2 copolymers with 0.1 mol% and 0.2 mol% in (A) HEPES and (B) PBS; PNF-COOH copolymers with 0.2 mol% and 0.8 mol% in (C) HEPES and (D) PBS.

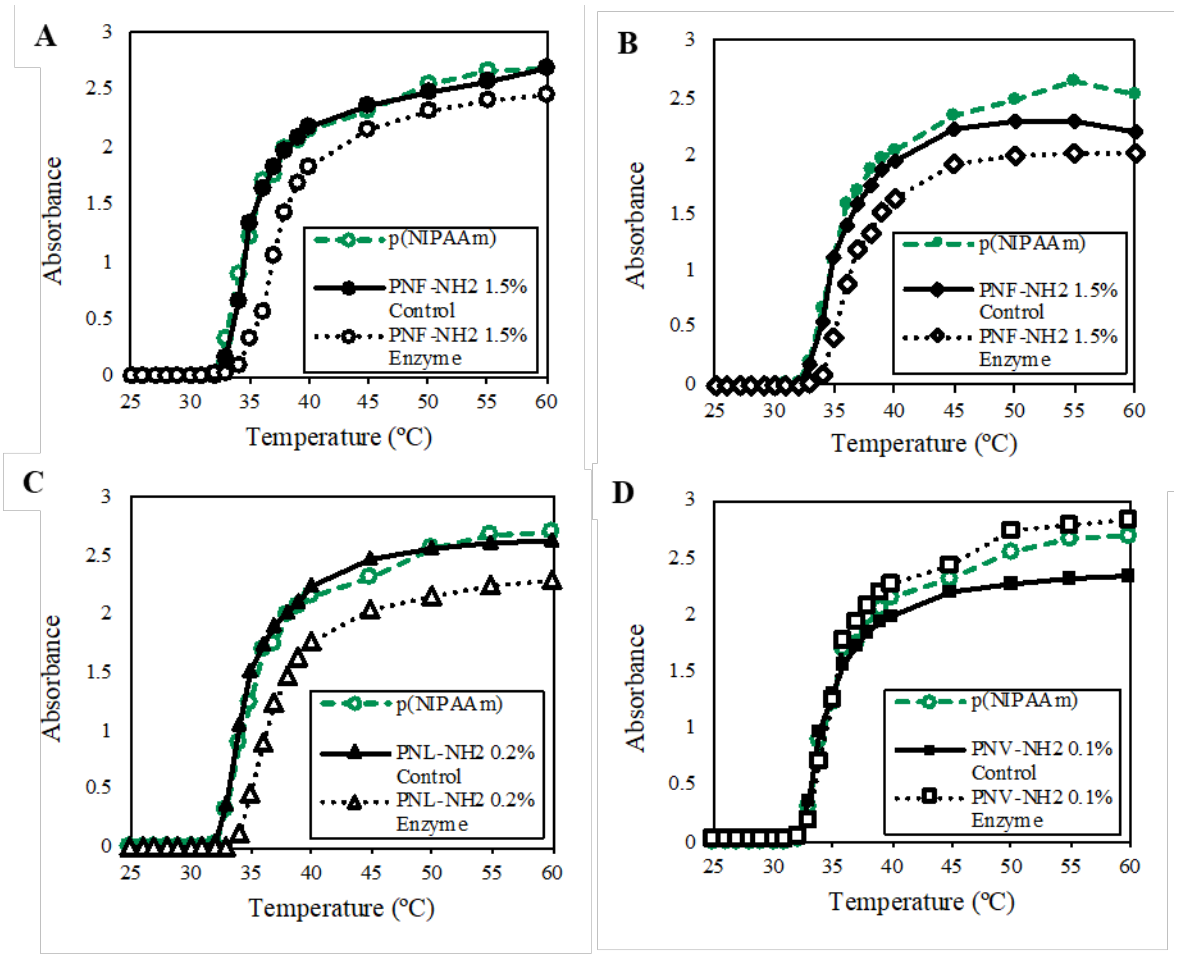

Figure 6. Relative absorbance at 450 nm before and after enzyme degradation of (A) PNF-NH_2 at 0.3 wt% in HEPES and (B) PNF-NH_2 at 0.3 wt% in PBS, (C) PNL-NH_2 at 0.3 wt% in HEPES, and (D) PNV-NH_2 at 0.3 wt% in HEPES.

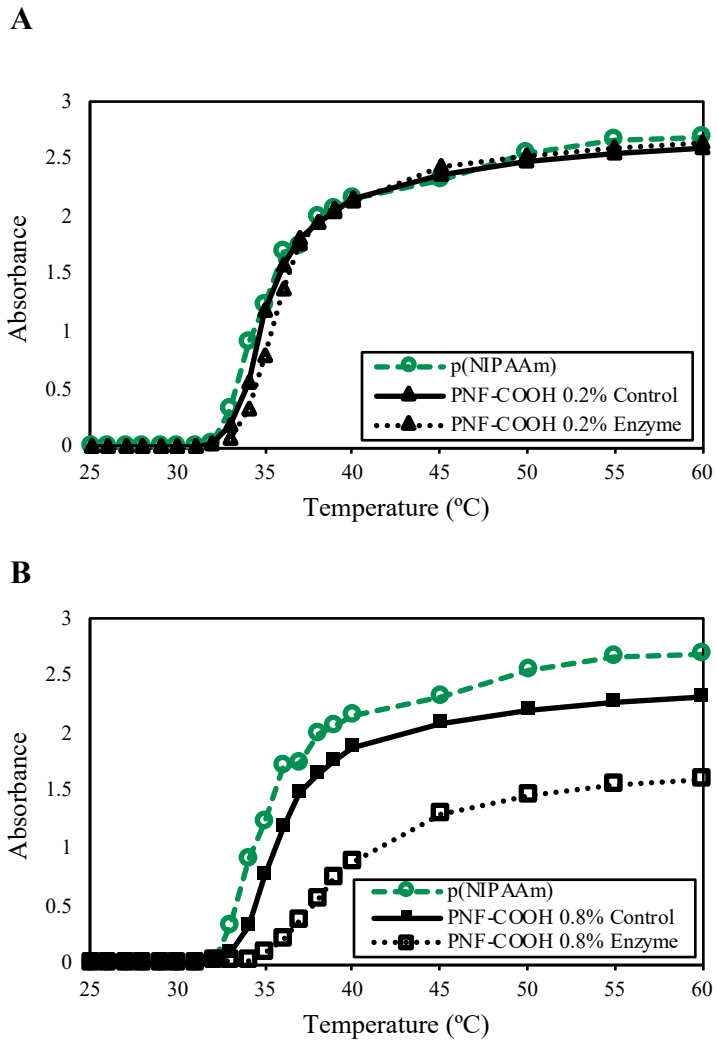

Figure 7. Relative absorbance at 450 nm of PNF-COOH with (A) 0.2 mol% and (B) 0.8 mol% peptide content before and after degradation at the polymer concentration of 0.3 wt% in HEPES.

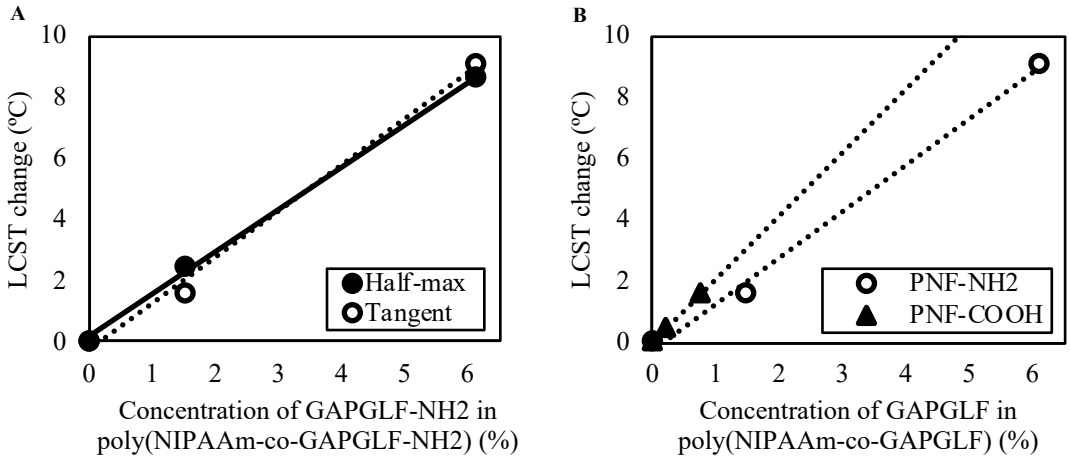

Figure 8. Variation of LCST due to enzyme degradation with peptide composition in (A) PNF-NH_2 by half-max and tangent method, and (B) PNF-NH_2 and PNF-COOH by tangent method.

2.3.3. Rheology

Storage (G') and loss (G'') moduli of 30 wt% PNF-NH_2, PNL-NH_2 and PNV- NH_2 gels in HEPES buffer were obtained by amplitude sweep under the constant frequency of 1 Hz (**Error! Reference source not found.**). Rheology was done to evaluate the mechanical stability of PNL-NH_2, PNV-NH_2 and PNF-NH_2. **Error! Reference source not found.** shows the strain dependence of storage (G') and loss modulus (G'') of the gels formed by 30 wt% polymer. Greater G' value than G'' indicated the formation of gel at 37 ºC. Storage moduli were reported in **Error! Reference source not found.** at 0.5% strain, where PNL-NH_2 and PNV-NH_2 samples exhibit a linear viscoelastic region at a small strain range (0.1-1%). PNF-NH_2 had the highest storage modulus at 72 kPa, as shown in Table 1. It also had the lowest cross-over strain, at 3% strain. The highest critical strain corresponded to PNL-NH_2 and PNV-NH_2 containing 0.1 mol% peptide, at 2% strain.

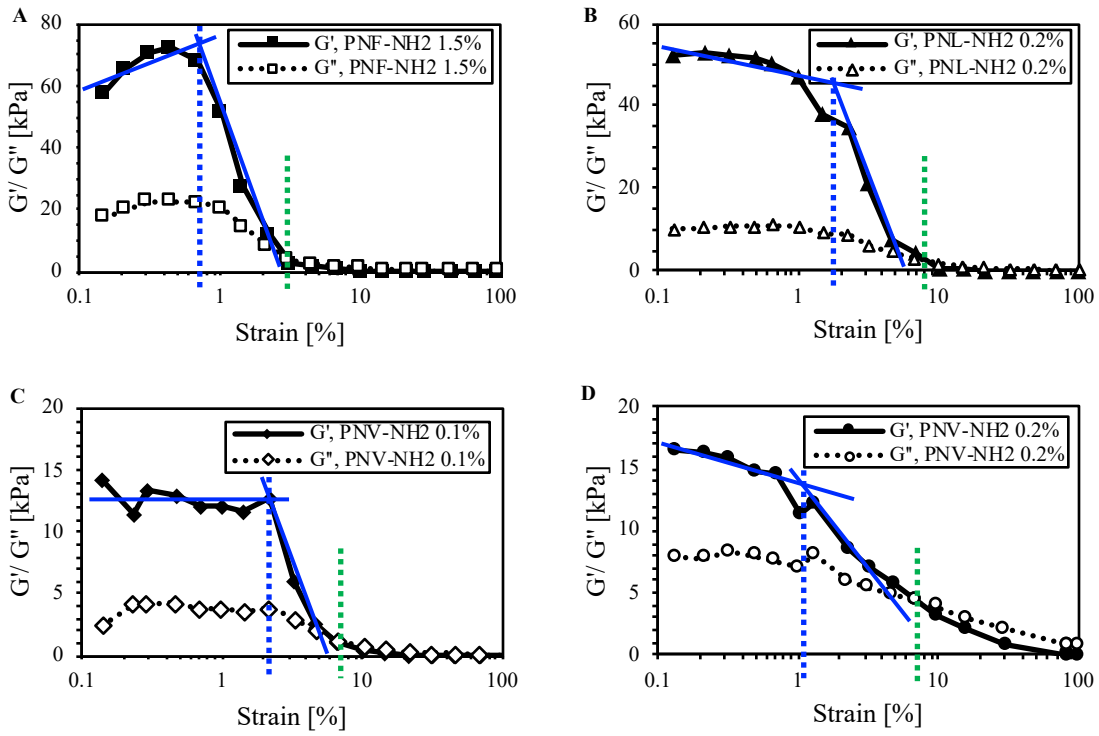

Figure 9. Storage modulus (G') and loss modulus (G'') vs applied strain for (A) PNF-NH_2, (B) PNL-NH_2, (C) PNV-NH_2 containing 0.1 mol% and (D) PNV-NH_2 containing 0.2 mol% peptide by amplitude sweep under the frequency of 1 Hz at the polymer concentration of 30 wt% in HEPES. In each graph, blue dotted line indicates critical strain and green dotted line indicates cross-over strain.

2.4. Discussion

Poly(NIPAAm-*co*-peptide) copolymers were synthesized according to previous literature[57], as shown on Scheme 2. Poly(NIPAAm-*co*-NASI) was synthesized by free radical polymerization, then peptide was conjugated. Then poly(NIPAAm-*co*-NASI-*co*-peptide) was synthesized by nucleophilic attack on the carbonyl group of NASI by the primary amine group of the peptide. Peptide conjugation was confirmed by the presence of peaks corresponding to the methyl protons of Leu, between ~0.9 ppm and ~1.0 ppm. Substitution of the remaining NASI by N-isopropylamine was confirmed by the absence of the ~2.89 ppm peak corresponding to the methylene protons of NASI as shown in

Figure **4**. Similarly, enzyme degradation was confirmed by the absence of the peak corresponding to the methyl protons of leucine as seen in **Error! Reference source not found.**, which suggests the cleavage of the Gly-Leu bond of the peptide.

PNF-NH_2 synthesized in previous literature with 4 mol% peptide in feed contained 6.1 mol% peptide, as seen in Table 1. This copolymer was dialyzed against 10 kDa MWCO, which may have eliminated smaller chains with less or no peptide content. We used 3.5 kDa MWCO during our purification process, so our peptide composition as determined by the ratio of NIPAAm to leucine in ^{1}H NMR spectra accounts for all the big as well as small chains of pNIPAAm copolymer, which upon counting, came up to contain little to no peptide. In order to confirm this theory, poly(NIPAAm-*co*-peptide) could be fractionated by dialysis and ^{1}H NMR could be used to determine if the higher molecular weight chains contain the most peptide.

LCST of all the copolymers was determined by tangent and half-max methods, as shown in

Table **2** and Table 3. In the tangent method, the calculated temperature is at which precipitation of the polymer starts occurring in the solution. The half-max method gives a good indication of heterogeneity, which may arise from polydispersity in molecular weight or peptide conjugation in the copolymers. Chains will precipitate at different temperatures according to their composition. Lower molecular weight chains will precipitate at lower temperatures.[59] Chains with higher peptide content before degradation will likely precipitate at lower temperatures, due to the hydrophobic nature of the peptides.[57] Likewise, after enzyme degradation, chains with higher peptide content will likely precipitate at higher temperatures due to the hydrophilic nature of the carboxylic acid termination in the peptide after degradation.[60] Using a 3.5 kDa MWCO dialysis bag likely resulted in heterogeneous copolymers, as seen from the LCST difference of 2 to 3 ºC of the copolymers before degradation calculated by half-max and tangent method (

Table **2** and Table 3). This heterogeneity could be reduced by using a higher MWCO dialysis bag, which would result in similar half-max and tangent LCST values.

It was observed that the change in LCST obtained by the half-max method (Table 2) differed from the tangent method change in LCST (Table 3) for PNL-NH_2, PNF-NH_2, and PNF-COOH, but not for PNV-NH_2, which suggests the heterogeneity of the PNL-NH_2, PNF-NH_2, and PNF-COOH. Also, this suggests that PNV-NH_2 containing 0.13 mol% peptide may be more homogeneous, which could be due to its lower peptide conjugation as compared to PNF-NH_2, and PNF-COOH. Both PNL-NH_2 and PNV-NH_2 had ~0.2 mol% peptide content, but Leu is more hydrophobic than Val, due to its extra methylene group, as shown in Figure 2. Therefore, the LCST of PNL-NH_2 (32 ºC) before degradation was lower than that of PNV-NH_2 (34 ºC). The LCST of PNL-NH_2 is also lower than pNIPAAm (32.6 ºC), which shows that the hydrophobicity of Leu was significant to lower the LCST at 0.2 mol% peptide content.

Enzyme degradation was carried out in two different buffer solutions containing calcium salt for the activation of collagenase for PNF-NH_2. Half-max LCST data in **Error! Reference source not found.** shows that the change in LCST was greater in HEPES as compared to PBS for PNF-NH_2, suggesting that the higher buffer concentration in PBS affected the LCST of PNF-NH_2 after degradation. . This result is consistent with previous work that has shown that higher buffer concentration lowers the LCST of p(NIPAAm) copolymers.[60,70] Dissolution of copolymers in water has to compete with that of the charged entities of buffer. Furthermore, inter/intra molecular hydrogen bonding complexes between carboxylic acid from GAPG-COOH and amide groups are favored, producing a lower LCST.[60] A way to determine if buffer strength affects the state of the copolymer chain after

degradation would be by dynamic light scattering (DLS), which would determine if the polymer dissolved in 150 mM PBS has a larger hydrodynamic diameter as compared to when dissolved in 125 mM HEPES. A larger size would correspond to the size of the aggregates formed by the polymer while in the globule state, as compared to the chains being in the coil state.[70]

Enzyme degradation was also carried out in HEPES containing calcium salt for PNL-NH_2, PNV-NH_2 containing 0.13 mol% peptide, and PNF-COOH copolymers. Cloud point data obtained indicates that LCST increases after enzymatic degradation for all copolymers, suggesting the conversion of poly(NIPAAm-*co*-GAPGLX) to the hydrophilic poly(NIPAAm-*co*-GAPG-COOH). Importantly, the highest LCST after degradation corresponds to the polymers with the highest initial peptide content. These polymers will have the greatest amount of GAPG-COOH, resulting in a greater LCST. The next step would be to investigate enzyme kinetics and compare across all copolymers.

Rheology of the polymer gels provide the information about G', critical strain and cross-over strain (Table 1). G' values depicts the mechanical stability of the gels; critical strain values show the strain at which the network structure would start getting disrupted and cross-over strain is the strain at which the material would start to flow. Past the cross-over strain, the copolymers could be deliverable through a catheter at 37ºC, as shown in Figure 9. This demonstrates that the gels are shear-thinning due to the physical crosslinking associated with pNIPAAm copolymers. Physical crosslinks of these gels at 30 wt% are disturbed between 0.6 and 2% strain and broken at 3% for PNF-NH_2 and at 7-8% for PNL-NH_2 and PNV-NH_2 copolymers. G' values indicated that PNF-NH_2 has the greatest

mechanical stability of all the gels and doubling of peptide content in PNV-NH_2 did not change its mechanical stability.

CHAPTER 3

CONCLUSION AND FUTURE WORK

3.1. Conclusion

A series of enzyme degradable NIPAAm based copolymers was successfully synthesized and characterized. Cloud point and ^{1}H NMR data suggest the cleavage of the Gly-Leu peptide bond by collagenase in HEPES buffer, converting the copolymers to poly(NIPAAm-*co*-GAPG-COOH). According to the literature and based on our research, increase in the peptide content in the copolymer makes it more prone to enzyme degradation, causing increase in the LCST of the copolymer after degradation. PNF-NH_2 had the greatest peptide conjugation success, and rheology data suggests that it also has the highest mechanical stability, which is crucial for liquid embolic agents. Hence, F-NH_2 showed the greatest potential for producing a mechanically stable liquid embolic agent that could attain a change in LCST to above body temperature upon degradation. Enzymatic degradation property and moderate mechanical stability convinces the use for these copolymers for endovascular embolization.

3.2. Future Work

3.2.1. Optimization of Peptide Substitution

Our study demonstrated the successful conjugation of NASI to NIPAAm. However, the nucleophilic substitution of NASI in P(NIPAAm-co-NASI) by the peptide needs optimization. Some insight could be gained by investigating the reaction kinetics of this nucleophilic substitution reaction, while varying the amount of TEA added to the reaction, the temperature at which the reaction proceeds, and solubilization of the peptide in reaction solvent. The addition of more TEA could increase the rate at which NASI gets substituted by the peptide, possibly shifting the reaction from 1st to 2nd order reaction, In first order reactions, the reaction slows down as the amount of reagent, in this case peptide, is reduced, while second order reactions are not as dependent on the amount of reagent left as the reaction proceeds. In addition, alternative methods to measure peptide content should be explored, due to the difficulty of accurately integrating the peaks corresponding to the peptide by NMR. Mass spectrometry has been used to quantify the peptide content in polymer-peptide copolymers[71,72] and may be useful for this application.

3.2.2. Incorporation of Cell-adhesive Peptides

Cell-adhesive peptides in hydrogels have shown improved cellular attachment, migration, and proliferation for a variety of cell types. [73,74] Peptides based on the Arg-Gly-Asp (RGD) sequence enable cell attachment by binding to integrin receptors that are present on the cell surface.[74,75] This peptide is derived from fibronectin, which is a cell-adhesive component of the extracellular matrix (ECM).[75] Cell adhesion strength of Gly-Arg-Gly-Asp-Ser (GRGDS) has been previously determined to be much higher than RGD. [73,76] Incorporation of cell-adhesive peptide GRGDS will positively impact cell survival, proliferation, and

migration of most adherent cells. Adhesion of integrins present in endothelial cells to RGD causes these cells to acquire a migratory phenotype and rebuild or form new blood vessels.[77] This would favor remodelling of the parent artery, closing blood flow access to an aneurysm, AVM or hypervascular tumor. The conjugation of GRGDS in conjunction to GAPGLX to NIPAAm will render an injectable copolymer that is enzyme-degradable in addition to cell-adhesive, resulting in poly(NIPAAm-*co*-GAPGLX-*co*-GRGDS) copolymers.

3.2.3. Differential Scanning Calorimetry

LCST values obtained by cloud point determination varied greatly between tangent and half-max methods, providing an inconsistent point of comparison. Furthermore, it has been shown that the LCST reported values are affected by polymer concentration and molecular weight when measured by cloud point.[68,69] Another way of determining LCST that is not affected by those variables is by differential scanning calorimetry (DSC). This method would provide a more consistent comparison of LCST before and after degradation among different peptide compositions. The temperature corresponding to the maximum of the endothermic peak is typically reported as the LCST, while the start of the same peak is referred to as the onset. [57,67]

3.2.4. Analysis of Thermo-responsive Gelation

Another way to measure the temperature at which the polymer transitions from soluble to insoluble is by investigating the temperature at which the polymer transitions from being in solution to a gel. A thermo-responsive gelation test could better predict if the polymer would be soluble in aqueous solution after degradation. This is important to determine if the polymer would redissolve into the bloodstream after degradation to prevent

fragmentation that could result in the unwanted occlusion of nearby vessels. The polymer concentration should be sufficient to form a gel, often greater than 30 wt%, therefore requiring a greater amount of sample as compared to LCST determination methods, which require a concentration between 0.1-1 wt%.[78] The tube inversion test and rheology are two methods by which the phase separation behavior can be studied in this class of polymers. The tube inversion test is widely used to determine the gelation of a polymer solution. The results from this study is highly dependent on concentration, heating method and tube dimensions.[79] For this method, the solution is placed in a tube or vial, heated at small increments and maintained at that temperature for a specified amount of time.[80] The tube is inverted at each temperature until reaching the temperature at which it is no longer in solution and has formed a gel with no visual flow.[81] Rheology can also be used to study the sol-gel transition of a polymer. This is done by temperature sweep test at an amplitude of strain within the linear region of the polymer at increasing temperatures. The gelation temperature is at the crossover between the storage modulus (G') and the loss modulus (G''); the polymer is considered a gel when G' is higher than G''.[81]

3.2.5. Swelling Testing

The thermo-responsive mechanism of pNIPAAm results in the exertion of aqueous solution from the material. This could have affected the rheology results; a material that shrinks more will show a higher storage modulus. Swelling testing will help determine if PNF-NH_2 is more mechanically stable independent of shrinking. In addition, deswelling could potentially result in long procedure times when delivering a considerable amount of material to the site, as would be the case for large aneurysms. It has been demonstrated that the addition of Jeffamine® M-1000 can control shrinking associated with the precipitation

of pNIPAAm.[82] In addition, swelling of the material after delivery is not ideal because it would exert force on the vessel wall, potentially leading to rupture and hemorrhage. It has been previously shown that the addition of hydrophobic monomers in pNIPAAm decreases the swelling of the polymer by decreasing its affinity for water caused by hydrophobic interactions.[83] Therefore, swelling could be minimized by the hydrophobic peptides studied in this work. The amount of GAPGLX peptide should be optimized to produce the desirable LCST change after degradation, as well as to produce the desirable polymer hydrophobicity needed to prevent swelling of the material at the embolization site.

3.2.6. Creep Resistance

A liquid embolic agent must be resistant to creep in response to constant stresses from blood flow. For applications in aneurysms, the material will be exposed to constant stress from blood flow. Therefore, additional mechanical testing should be done to ensure it is resistant to creep under a constant shear stress. The addition of hydrophobic segments has been shown to increase shear and creep strength of hydrogels.[57,84] Hence, GAPGLX peptides may also contribute to creep resistance. The addition of chemical crosslinks may also increase its mechanical stability and creep resistance due to the elasticity associated with chemical crosslinking.[58] Acrylate groups attached to the end of the peptide will enable these copolymers to chemically crosslink with thiols present in pentaerythritol tetrakis (3-mercaptopropionate) (QT) in aqueous solution by Michael-addition. [85–89] Thus, resulting in dual physically and chemically crosslinked poly(NIPAAm-*co*-GAPGLX-*co*-GRGDS-Ac)/QT copolymers that are mechanically stable, bioactive, and enzyme-degradable for endovascular embolization.

REFERENCES

(1) Rautio, R.; Haapanen, A. Transcatheter Embolization of a Renal Artery Aneurysm Using Ethylene Vinyl Alcohol Copolymer. *Cardiovasc. Intervent. Radiol.* **2007**, *30* (2), 300–303. https://doi.org/10.1007/s00270-005-0238-2.

(2) Dawbarn, R. H. M. The Starvation Operation for Malignancy in the External Carotid Area: Its Failures and Successes. *JAMA J. Am. Med. Assoc.* **1904**, *XLIII* (12), 792. https://doi.org/10.1001/jama.1904.92500120002g.

(3) Luessenhop, A. J. Artificial Embolization of Cerebral Arteries. *J. Am. Med. Assoc.* **1960**, *172* (11), 1153. https://doi.org/10.1001/jama.1960.63020110001009.

(4) Serbinenko, F. A. Occlusion of the Cavernous Portion of the Carotid Artery with a Balloon as a Method of Treating Carotid-Cavernous Anastomosis. *Vopr. Neirokhir.* **1971**, *35* (6), 3–9.

(5) Dolmatch Bart L. The History of CT Angiography. *Endovasc. Today* **2005**, No. July, 23–30.

(6) Djindjian, R.; Cophignon, J.; Rey, A.; Théron, J.; Merland, J. J.; Houdart, R. Superselective Arteriographic Embolization by the Femoral Route in Neuroradiology. Study of 50 Cases. II. Embolization in Vertebromedullary Pathology. *Neuroradiology* **1973**, *6* (3), 132–142.

(7) Kricheff, I. I.; Madayag, M.; Braunstein, P. Transfemoral Catheter Embolization of Cerebral and Posterior Fossa Arteriovenous Malformations. *Radiology* **1972**, *103* (1), 107–111. https://doi.org/10.1148/103.1.107.

(8) Rösch, J.; Dotter, C. T.; Brown, M. J. Selective Arterial Embolization. A New Method for Control of Acute Gastrointestinal Bleeding. *Radiology* **1972**, *102* (2), 303–306. https://doi.org/10.1148/102.2.303.

(9) Hilal, S. K.; Michelsen, J. W. Therapeutic Percutaneous Embolization for Extra-Axial Vascular Lesions of the Head, Neck, and Spine. *J. Neurosurg.* **1975**, *43* (3), 275–287. https://doi.org/10.3171/jns.1975.43.3.0275.

(10) Jordan, O.; Doelker, E.; Rüfenacht, D. A. Biomaterials Used in Injectable Implants (Liquid Embolics) for Percutaneous Filling of Vascular Spaces. *Cardiovasc. Intervent. Radiol.* **2005**, *28* (5), 561–569. https://doi.org/10.1007/s00270-004-0238-7.

(11) Cromwell, L.; Kerber, C. Modification of Cyanoacrylate for Therapeutic Embolization: Preliminary Experience. *Am. J. Roentgenol.* **1979**, *132* (5), 799–801. https://doi.org/10.2214/ajr.132.5.799.

(12) Brassel, F.; Meila, D. Evolution of Embolic Agents in Interventional Neuroradiology. *Clin. Neuroradiol.* **2015**, *25*, 333–339. https://doi.org/10.1007/s00062-015-0419-6.

(13) Gianturco, C.; Anderson, J. H.; Wallace, S. Mechanical Devices for Arterial Occlusion. *Am. J. Roentgenol.* **1975**, *124* (3), 428–435. https://doi.org/10.2214/ajr.124.3.428.

(14) Guglielmi, G.; Viñuela, F.; Sepetka, I.; Macellari, V. Electrothrombosis of Saccular Aneurysms via Endovascular Approach. Part 1: Electrochemical Basis, Technique, and Experimental Results. *J. Neurosurg.* **1991**, *75* (1), 1–7. https://doi.org/10.3171/jns.1991.75.1.0001.

(15) Dalyai, R. T. Z.; Schirmer, C. M.; Malek, A. M. Transvenous Balloon-Protected Embolization of a Scalp Arteriovenous Fistula Using Onyx Liquid Embolic. *Acta Neurochir. (Wien).* **2011**, *153* (6), 1285–1290. https://doi.org/10.1007/s00701-011-0998-1.

(16) Helmy, A.; Shaida, N. Treatment of Type II Endoleaks with a Novel Agent: Precipitating Hydrophobic Injectable Liquid (PHIL). *Cardiovasc. Intervent. Radiol.* **2017**, *40* (7), 1094–1098. https://doi.org/10.1007/s00270-017-1603-7.

(17) Lamin, S.; Chew, H. S.; Chavda, S.; Thomas, A.; Piano, M.; Quilici, L.; Pero, G.; Holtmannspolter, M.; Cronqvist, M. E.; Casasco, A.; et al. Embolization of Intracranial Dural Arteriovenous Fistulas Using PHIL Liquid Embolic Agent in 26 Patients: A Multicenter Study. *AJNR. Am. J. Neuroradiol.* **2017**, *38* (1), 127–131. https://doi.org/10.3174/ajnr.A5037.

(18) AANS. Arteriovenous Malformations https://www.aans.org/Patients/Neurosurgical-Conditions-and-Treatments/Arteriovenous-Malformations.

(19) Dunham, G. M.; Ingraham, C. R.; Maki, J. H.; Vaidya, S. S. Finding the Nidus: Detection and Workup of Non–Central Nervous System Arteriovenous Malformations. *RadioGraphics* **2016**, *36* (3), 891–903. https://doi.org/10.1148/rg.2016150177.

(20) Wang, X.; Wang, Q.; Chen, G.; Leng, B.; Song, D. Endovascular Treatment of Congenital Brain Arteriovenous Fistulas with Combination of Detachable Coils and Onyx Liquid Embolic Agent. *Neuroradiology* **2010**, *52* (12), 1121–1126. https://doi.org/10.1007/s00234-010-0681-x.

(21) Vollherbst, D. F.; Sommer, C. M.; Ulfert, C.; Pfaff, J.; Bendszus, M.; Möhlenbruch, M. A. Liquid Embolic Agents for Endovascular Embolization: Evaluation of an Established (Onyx) and a Novel (PHIL) Embolic Agent in an in Vitro AVM Model. *Am. J. Neuroradiol.* **2017**, *38* (7), 1377–1382. https://doi.org/10.3174/ajnr.A5203.

(22) Blackburn, S. L.; Kadkhodayan, Y.; Ray, W. Z.; Zipfel, G. J.; Cross, D. W. T.; Moran, C. J.; Derdeyn, C. P. Onyx Is Associated with Poor Venous Penetration in the Treatment of Spinal Dural Arteriovenous Fistulas. *J. Neurointerv. Surg.* **2014**, *6* (7). https://doi.org/10.1136/neurintsurg-2013-010779.

(23) Kocer, N.; Hanimoglu, H.; Batur, S.; Kandemirli, S. G.; Kizilkilic, O.; Sanus, Z.; Oz, B.; Islak, C.; Kaynar, M. Y. Preliminary Experience with Precipitating Hydrophobic Injectable Liquid in Brain Arteriovenous Malformations. *Diagnostic Interv. Radiol.* **2016**, *22* (2), 184–189. https://doi.org/10.5152/dir.2015.15283.

(24) Taki, W.; Yonekawa, Y.; Iwata, H.; Uno, A.; Yamashita, K.; Amemiya, H. A New Liquid Material for Embolization of Arteriovenous Malformations. *AJNR. Am. J. Neuroradiol. 11* (1), 163–168.

(25) Johnson, C. S.; Chiu, A.; Cheung, A.; Wenderoth, J. Embolization of Cranial Dural Arteriovenous Fistulas in the Liquid Embolic Era: A Sydney Experience. *J. Clin. Neurosci.* **2018**, *49*, 62–70. https://doi.org/10.1016/J.JOCN.2017.12.007.

(26) Brain Aneurysm Foundation. Statistics and Facts of Brain Aneurysms https://bafound.org/about-brain-aneurysms/brain-aneurysm-basics/brain-aneurysm-statistics-and-facts/.

(27) Weber, W.; Siekmann, R.; Kis, B.; Kuehne, D. Treatment and Follow-up of 22 Unruptured Wide-Necked Intracranial Aneurysms of the Internal Carotid Artery with Onyx HD 500. *AJNR. Am. J. Neuroradiol.* **2005**, *26* (8), 1909–1915.

(28) Kim, J.-W.; Park, Y.-S. Endovascular Treatment of Wide-Necked Intracranial Aneurysms : Techniques and Outcomes in 15 Patients. *J. Korean Neurosurg. Soc.* **2011**, *49* (2), 97–101. https://doi.org/10.3340/jkns.2011.49.2.97.

(29) Eddleman, C. S.; Surdell, D.; DiPatri, A.; Tomita, T.; Shaibani, A. Infectious Intracranial Aneurysms in the Pediatric Population: Endovascular Treatment with Onyx. *Child's Nerv. Syst.* **2008**, *24* (8), 909–915. https://doi.org/10.1007/s00381-008-0614-8.

(30) Khaja, M. S.; Park, A. W.; Swee, W.; Evans, A. J.; Fritz Angle, J.; Turba, U. C.; Sabri, S. S.; Matsumoto, A. H. Treatment of Type II Endoleak Using Onyx with Long-Term Imaging Follow-Up. *Cardiovasc. Intervent. Radiol.* **2014**, *37* (3), 613–622. https://doi.org/10.1007/s00270-013-0706-z.

(31) Fusco, M. R.; Salem, M. M.; Gross, B. A.; Reddy, A. S.; Ogilvy, C. S.; Kasper, E. M.; Thomas, A. J. Preoperative Embolization of Extra-Axial Hypervascular Tumors with Onyx. *J. Cerebrovasc. Endovasc. Neurosurg.* **2016**, *18* (1), 12. https://doi.org/10.7461/jcen.2016.18.1.12.

(32) Clarençon, F.; Di Maria, F.; Cormier, E.; Sourour, N.-A.; Enkaoua, E.; Sailhan, F.; Iosif, C.; Le Jean, L.; Chiras, J. Onyx Injection by Direct Puncture for the Treatment of Hypervascular Spinal Metastases Close to the Anterior Spinal Artery: Initial Experience. *J. Neurosurg. Spine* **2013**, *18* (6), 606–610. https://doi.org/10.3171/2013.3.SPINE12832.

(33) Trivelatto, F.; Nakiri, G. S.; Manisor, M.; Riva, R.; Al-Khawaldeh, M.; Kessler, I.; Mounayer, C. Preoperative Onyx Embolization of Meningiomas Fed by the Ophthalmic Artery: A Case Series. *Am. J. Neuroradiol.* **2011**, *32* (9), 1762–1766. https://doi.org/10.3174/ajnr.A2591.

(34) Poursaid, A.; Jensen, M. M.; Huo, E.; Ghandehari, H. Polymeric Materials for Embolic and Chemoembolic Applications. *J. Control. Release* **2016**, *240*, 414–433. https://doi.org/10.1016/j.jconrel.2016.02.033.

(35) Pollak, J. S.; White, R. I. The Use of Cyanoacrylate Adhesives in Peripheral Embolization. *J. Vasc. Interv. Radiol.* **2001**, *12* (8), 907–913.

(36) Kumaran, S.; Nambi, G. I.; Gupta, A. K. Preventable Complication after Glue Sclerotherapy for Scalp Arteriovenous Malformation. *J. Plast. Reconstr. Aesthetic Surg.* **2008**, *61* (7), 854–855. https://doi.org/10.1016/j.bjps.2008.04.008.

(37) Paramasivam, S.; Niimi, Y.; Fifi, J.; Berenstein, A. Onyx Embolization Using Dual-Lumen Balloon Catheter: Initial Experience and Technical Note. *J. Neuroradiol.* **2013**, *40* (4), 294–302. https://doi.org/10.1016/j.neurad.2013.08.001.

(38) Cobb, R. J.; Patterson, B.; Karthikesalingam, A.; Morgan, R.; Thompson, M.; Loftus, I. Onyx: A Novel Solution for a Mycotic Aneurysm. *Cardiovasc. Intervent. Radiol.* **2014**, *37* (2), 541–543. https://doi.org/10.1007/s00270-013-0604-4.

(39) Gentric, J. C.; Raymond, J.; Batista, A.; Salazkin, I.; Gevry, G.; Darsaut, T. E. Dual-Lumen Balloon Catheters May Improve Liquid Embolization of Vascular Malformations: An Experimental Study in Swine. *AJNR. Am. J. Neuroradiol.* **2015**, *36* (5), 977–981. https://doi.org/10.3174/ajnr.A4211.

(40) Patel, A. S.; Horton, T. G.; Kalapos, P.; Cockroft, K. M. Onyx-HD 500 Embolization of a Traumatic Internal Carotid Artery Pseudoaneurysm after Transsphenoidal Surgery. *J. Neuroimaging* **2015**, *25* (4), 656–659. https://doi.org/10.1111/jon.12221.

(41) Saeed Kilani, M.; Izaaryene, J.; Cohen, F.; Varoquaux, A.; Gaubert, J. Y.; Louis, G.; Jacquier, A.; Bartoli, J. M.; Moulin, G.; Vidal, V. Ethylene Vinyl Alcohol Copolymer (Onyx®) in Peripheral Interventional Radiology: Indications, Advantages and Limitations. *Diagn. Interv. Imaging* **2015**, *96* (4), 319–326. https://doi.org/10.1016/j.diii.2014.11.030.

(42) Gross, B. A.; Albuquerque, F. C.; Moon, K.; McDougall, C. G. Evolution of Treatment and a Detailed Analysis of Occlusion, Recurrence, and Clinical Outcomes in an Endovascular Library of 260 Dural Arteriovenous Fistulas. *J. Neurosurg.* **2016**, 1884–1893. https://doi.org/10.3171/2016.5.JNS16331.

(43) Gobin, Y. P.; Murayama, Y.; Milanese, K.; Chow, K.; Gonzalez, N. R.; Duckwiler, G. R.; Viñuela, F. Head and Neck Hypervascular Lesions: Embolization with Ethylene Vinyl Alcohol Copolymer—Laboratory Evaluation in Swine and Clinical Evaluation in Humans. *Radiology* **2001**, *221* (2), 309–317. https://doi.org/10.1148/radiol.2212001140.

(44) Choo, D. M.; Shankar, J. J. S. Onyx versus NBCA and Coils in the Treatment of Intracranial Dural Arteriovenous Fistulas. *Interv. Neuroradiol.* **2016**, *22* (2), 212–216. https://doi.org/10.1177/1591019915622170.

(45) Natarajan, S. K.; Born, D.; Ghodke, B.; Britz, G. W.; Sekhar, L. N. Histopathological Changes in Brain Arteriovenous Malformations after Embolization Using Onyx or N-Butyl Cyanoacrylate. *J. Neurosurg.* **2009**, 105–113. https://doi.org/10.3171/2008.12.JNS08441.

(46) Smith, S. J.; Thomas, A.; Ashpole, R. D. Intra-Operative Combustion of Onyx Embolic Material. *Br. J. Neurosurg.* **2009**, *23* (1), 76–78. https://doi.org/10.1080/02688690802512866.

(47) Murayama, Y.; Viñuela, F.; Ulhoa, A.; Akiba, Y.; Duckwiler, G. R.; Gobin, Y. P.; Vinters, H. V; Greff, R. J. Nonadhesive Liquid Embolic Agent for Cerebral Arteriovenous Malformations: Preliminary Histopathological Studies in Swine Rete Mirabile. *Neurosurgery* **1998**, *43* (5), 1164–1175.

(48) Hartmann, A.; Pile-Spellman, J.; Stapf, C.; Sciacca, R. R.; Faulstich, A.; Mohr, J. P.; Schumacher, H. C.; Mast, H. Risk of Endovascular Treatment of Brain Arteriovenous Malformations. *Stroke* **2002**, *33* (7), 1816–1820.

(49) Berenstein, A. Treatment of Experimental Aneurysms with a New Liquid Embolic Agent and a Retrievable Stent: Proof of Concept and Feasibility Study. *J. Neurointerv. Surg.* **2015**, *8* (9), 934–939. https://doi.org/10.1136/neurintsurg-2015-011930.

(50) Varadharajan, S.; Ramalingaiah, A. H.; Saini, J.; Gupta, A. K.; Devi, B. I.; Acharya, U. V. Precipitating Hydrophobic Injectable Liquid Embolization of Intracranial Vascular Shunts: Initial Experience and Technical Note. *J. Neurosurg.* **2017**, 1–6. https://doi.org/10.3171/2017.6.JNS16447.

(51) Vaidya, S.; Tozer, K.; Chen, J. An Overview of Embolic Agents. *Semin. Intervent. Radiol.* **2008**, *25* (03), 204–215. https://doi.org/10.1055/s-0028-1085930.

(52) Orozco, L. D.; Luzardo, G. D.; Buciuc, R. F. Transarterial Balloon Assisted Onyx Embolization of Pericallosal Arteriovenous Malformations. *J. Neurointerv. Surg.* **2013**, *5* (4), e18. https://doi.org/10.1136/neurintsurg-2012-010388.

(53) Jagadeesan, B. D.; Grigoryan, M.; Hassan, A. E.; Grande, A. W.; Tummala, R. P. Endovascular Balloon-Assisted Embolization of Intracranial and Cervical Arteriovenous Malformations Using Dual-Lumen Coaxial Balloon Microcatheters and Onyx: Initial Experience. *Neurosurgery* **2013**, *73* (2 Suppl Operative), ons238–43; discussion ons243. https://doi.org/10.1227/NEU.0000000000000186.

(54) Park, S. Compliant Neurovascular Balloon Catheters May Not Be Compatible with Liquid Embolic Materials: Intraprocedural Rupture of the Protecting Balloon during Tumor Embolization Using n-Butyl Cyanoacrylate and Lipiodol Mixture. *J. Neurointerv. Surg.* **2015**, *7* (10), 740–744.

(55) Scarpa, J. S.; Mueller, D. D.; Klotz, I. M. Slow Hydrogen-Deuterium Exchange in a Non-.Alpha.-Helical Polyamide. *J. Am. Chem. Soc.* **1967**, *89* (24), 6024–6030. https://doi.org/10.1021/ja01000a006.

(56) Malikmammadov, E.; Hasirci, N. Dual- and Multistimuli-Responsive Polymers for Biomedical Applications. In *Smart Polymers and their Applications*; Elsevier, 2019; pp 255–278. https://doi.org/10.1016/B978-0-08-102416-4.00008-9.

(57) Overstreet, D. J.; Dhruv, H. D.; Vernon, B. L. Bioresponsive Copolymers of Poly(N-Isopropylacrylamide) with Enzyme-Dependent Lower Critical Solution Temperatures. *Biomacromolecules* **2010**, *11* (5), 1154–1159. https://doi.org/10.1021/bm100035f.

(58) Overstreet, D. J. Temperature-Responsive Hydrogels with Controlled Water Content and Their Development toward Drug Delivery and Embolization Applications, Arizona State University, 2012.

(59) Plunkett, K. N.; Zhu, X.; Moore, J. S.; Leckband, D. E. PNIPAM Chain Collapse Depends on the Molecular Weight and Grafting Density. *Langmuir* **2006**, *22* (9), 4259–4266. https://doi.org/10.1021/la0531502.

(60) Minoo-Rabeeh–Hobabi; Hassanzadeh, D.; Azarmi, S.; Entezami, A. A. Effect of Synthesis Method and Buffer Composition on the LCST of a Smart Copolymer OfN-Isopropylacrylamide and Acrylic Acid. *Polym. Adv. Technol.* **2007**, *18* (12), 986–992. https://doi.org/10.1002/pat.951.

(61) Lemanowicz, M.; Gierczycki, A.; Kuźnik, W.; Sancewicz, R.; Imiela, P. Determination of Lower Critical Solution Temperature of Thermosensitive Flocculants. *Miner. Eng.* **2014**, *69*, 170–176. https://doi.org/10.1016/j.mineng.2014.07.022.

(62) Boutris, C.; Chatzi, E. G.; Kiparissides, C. Characterization of the LCST Behaviour of Aqueous Poly(N-Isopropylacrylamide) Solutions by Thermal and Cloud Point Techniques. *Polymer (Guildf).* **1997**, *38* (10), 2567–2570. https://doi.org/10.1016/S0032-3861(97)01024-0.

(63) Yoshioka, H.; Mikami, M.; Mori, Y.; Tsuchida, E. A Synthetic Hydrogel with Thermoreversible Gelation. I. Preparation and Rheological Properties. *J. Macromol. Sci. Part A* **1994**, *31* (1), 113–120. https://doi.org/10.1080/10601329409349722.

(64) Kim, S.; Chung, E. H.; Gilbert, M.; Healy, K. E. Synthetic MMP-13 Degradable ECMs Based on Poly(N-Isopropylacrylamide-Co-Acrylic Acid) Semi-Interpenetrating Polymer Networks. I. Degradation and Cell Migration. *J. Biomed. Mater. Res. A* **2005**, *75* (1), 73–88. https://doi.org/10.1002/jbm.a.30375.

(65) Katayama, Y.; Sonoda, T.; Maeda, M. A Polymer Micelle Responding to the Protein Kinase A Signal. *Macromolecules* **2001**, *34* (24), 8569–8573. https://doi.org/10.1021/ma010966a.

(66) Page-McCaw, A.; Ewald, A. J.; Werb, Z. Matrix Metalloproteinases and the Regulation of Tissue Remodelling. *Nat. Rev. Mol. Cell Biol.* **2007**, *8* (3), 221–233. https://doi.org/10.1038/nrm2125.

(67) Fares, M. M.; Othman, A. A. Lower Critical Solution Temperature Determination of Smart, Thermosensitive N -Isopropylacrylamide- Alt -2-Hydroxyethyl Methacrylate Copolymers: Kinetics and Physical Properties. *J. Appl. Polym. Sci.* **2008**, *110* (5), 2815–2825. https://doi.org/10.1002/app.28840.

(68) Aseyev, V.; Tenhu, H.; Winnik, F. M. Non-Ionic Thermoresponsive Polymers in Water; 2010; pp 29–89. https://doi.org/10.1007/12_2010_57.

(69) Schroffenegger, M.; Reimhult, E. Thermoresponsive Core-Shell Nanoparticles and Their Potential Applications. In *Comprehensive Nanoscience and Nanotechnology*; Elsevier, 2019; pp 145–170. https://doi.org/10.1016/B978-0-12-803581-8.10431-X.

(70) Taha, M.; Gupta, B. S.; Khoiroh, I.; Lee, M.-J. Interactions of Biological Buffers with Macromolecules: The Ubiquitous "Smart" Polymer PNIPAM and the Biological Buffers MES, MOPS, and MOPSO. *Macromolecules* **2011**, *44* (21), 8575–8589. https://doi.org/10.1021/ma201790c.

(71) Sallam, S.; Dolog, I.; Paik, B. A.; Jia, X.; Kiick, K. L.; Wesdemiotis, C. Sequence and Conformational Analysis of Peptide–Polymer Bioconjugates by Multidimensional Mass Spectrometry. *Biomacromolecules* **2018**, *19* (5), 1498–1507. https://doi.org/10.1021/acs.biomac.7b01694.

(72) Alalwiat, A.; Grieshaber, S. E.; Paik, B. A.; Kiick, K. L.; Jia, X.; Wesdemiotis, C. Top-down Mass Spectrometry of Hybrid Materials with Hydrophobic Peptide and Hydrophilic or Hydrophobic Polymer Blocks. *Analyst* **2015**, *140* (22), 7550–7564. https://doi.org/10.1039/C5AN01600B.

(73) Idota, N.; Ebara, M.; Kotsuchibashi, Y.; Narain, R.; Aoyagi, T. Novel Temperature-Responsive Polymer Brushes with Carbohydrate Residues Facilitate Selective Adhesion and Collection of Hepatocytes. *Sci. Technol. Adv. Mater.* **2012**, *13* (6), 064206. https://doi.org/10.1088/1468-6996/13/6/064206.

(74) El-Sherbiny, I. M.; Yacoub, M. H. Hydrogel Scaffolds for Tissue Engineering: Progress and Challenges. *Glob. Cardiol. Sci. Pract.* **2013**, *2013* (3), 38. https://doi.org/10.5339/gcsp.2013.38.

(75) Ulijn, R. V.; Bibi, N.; Jayawarna, V.; Thornton, P. D.; Todd, S. J.; Mart, R. J.; Smith, A. M.; Gough, J. E. Bioresponsive Hydrogels. *Mater. Today* **2007**, *10* (4), 40–48. https://doi.org/10.1016/S1369-7021(07)70049-4.

(76) Sun, Y.; Kim, D.-H.; Simmons, C. A. *Integrative Mechanobiology*, 1st ed.; Cambridge University Press: Cambridge, United Kingdom, 2015.

(77) Le Saux, G.; Magenau, A.; Böcking, T.; Gaus, K.; Gooding, J. J. The Relative Importance of Topography and RGD Ligand Density for Endothelial Cell Adhesion. *PLoS One* **2011**, *6* (7), e21869. https://doi.org/10.1371/journal.pone.0021869.

(78) Constantin, M.; Cristea, M.; Ascenzi, P.; Fundueanu, G. Lower Critical Solution Temperature versus Volume Phase Transition Temperature in Thermoresponsive Drug Delivery Systems. *Express Polym. Lett.* **2011**, *5* (10), 839–848. https://doi.org/10.3144/expresspolymlett.2011.83.

(79) Singh, T. R. R.; Laverty, G.; Donelly, R. *Hydrogels: Design, Synthesis and Application in Drug Delivery and Regenerative Medicine*, 1st ed.; CRC Press: London, 2018.

(80) Gioffredi, E.; Boffito, M.; Calzone, S.; Giannitelli, S. M.; Rainer, A.; Trombetta, M.; Mozetic, P.; Chiono, V. Pluronic F127 Hydrogel Characterization and Biofabrication in Cellularized Constructs for Tissue Engineering Applications. *Procedia CIRP* **2016**, *49*, 125–132. https://doi.org/10.1016/j.procir.2015.11.001.

(81) Maeda, T.; Kitagawa, M.; Hotta, A.; Koizumi, S. Thermo-Responsive Nanocomposite Hydrogels Based on PEG-b-PLGA Diblock Copolymer and Laponite. *Polymers (Basel).* **2019**, *11* (2), 250. https://doi.org/10.3390/polym11020250.

(82) Caplan, M.; Mclaren, A. Temperature-Responsive Hydrogels with Controlled Water Content and Their Development Toward Drug Delivery and Embolization Applications by Derek Overstreet A Dissertation Presented in Partial Fulfillment of the Requirements for the Degree Doctor of Philos. **2012**, No. August.

(83) Lee, W.-F.; Yuan, W.-Y. Thermoreversible Hydrogels. XV. Swelling Behaviors and Drug Release for Thermoreversible Hydrogels Containing Silane Monomers. *J. Appl. Polym. Sci.* **2002**, *84* (13), 2523–2532. https://doi.org/10.1002/app.10561.

(84) Thomas, B. H.; Craig Fryman, J.; Liu, K.; Mason, J. Hydrophilic-Hydrophobic Hydrogels for Cartilage Replacement. *J. Mech. Behav. Biomed. Mater.* **2009**, *2* (6), 588–595. https://doi.org/10.1016/j.jmbbm.2008.08.001.

(85) Brennecka, C. R.; Preul, M. C.; Vernon, B. L. In Vitro Delivery, Cytotoxicity, Swelling, and Degradation Behavior of a Liquid-to-Solid Gelling Polymer System for Cerebral Aneurysm Embolization. *J. Biomed. Mater. Res. - Part B Appl. Biomater.* **2012**, *100 B* (5), 1298–1309. https://doi.org/10.1002/jbm.b.32696.

(86) Riley, C. M.; McLemore, R.; Preul, M. C.; Vernon, B. L. Gelling Process Differences in Reverse Emulsion, in Situ Gelling Polymeric Materials for Intracranial Aneurysm Embolization, Formulated with Injectable Contrast Agents. *J. Biomed. Mater. Res. - Part B Appl. Biomater.* **2011**, *96 B* (1), 47–56. https://doi.org/10.1002/jbm.b.31729.

(87) Brennecka, C. R.; Preul, M. C.; Becker, T. A.; Vernon, B. L. In Vivo Embolization of Lateral Wall Aneurysms in Canines Using the Liquid-to-Solid Gelling PPODA-QT Polymer System: 6-Month Pilot Study. *J. Neurosurg.* **2013**, *119* (1), 228–238. https://doi.org/10.3171/2013.3.JNS121865.

(88) Robb, S. A.; Lee, B. H.; McLemore, R.; Vernon, B. L. Simultaneously Physically and Chemically Gelling Polymer System Utilizing a Poly(NIPAAm-Co-Cysteamine)-Based Copolymer. *Biomacromolecules* **2007**, *8* (7), 2294–2300. https://doi.org/10.1021/bm070267r.

(89) McLemore, R. The Development of an in Situ-Gelling Reverse Emulsion Polymeric System for Functional Embolization, Arizona State University, 2007.

APPENDIX A

^{1}H NMR Spectra of Synthesized Copolymers

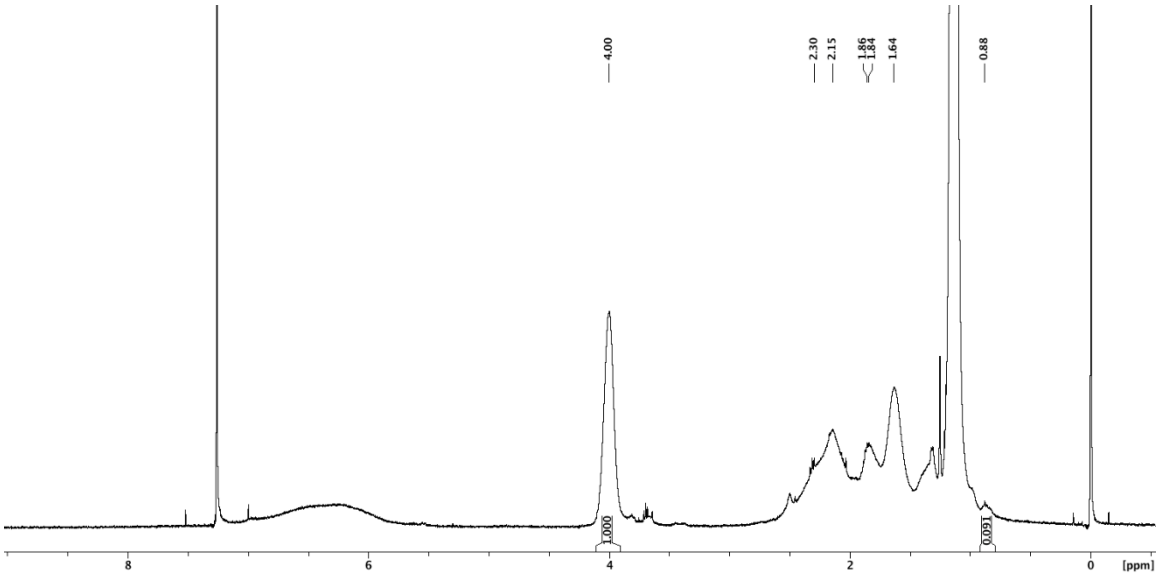

Figure 10. ^{1}H NMR spectrum of poly(NIPAAm-*co*-GAPGLF-NH_2).

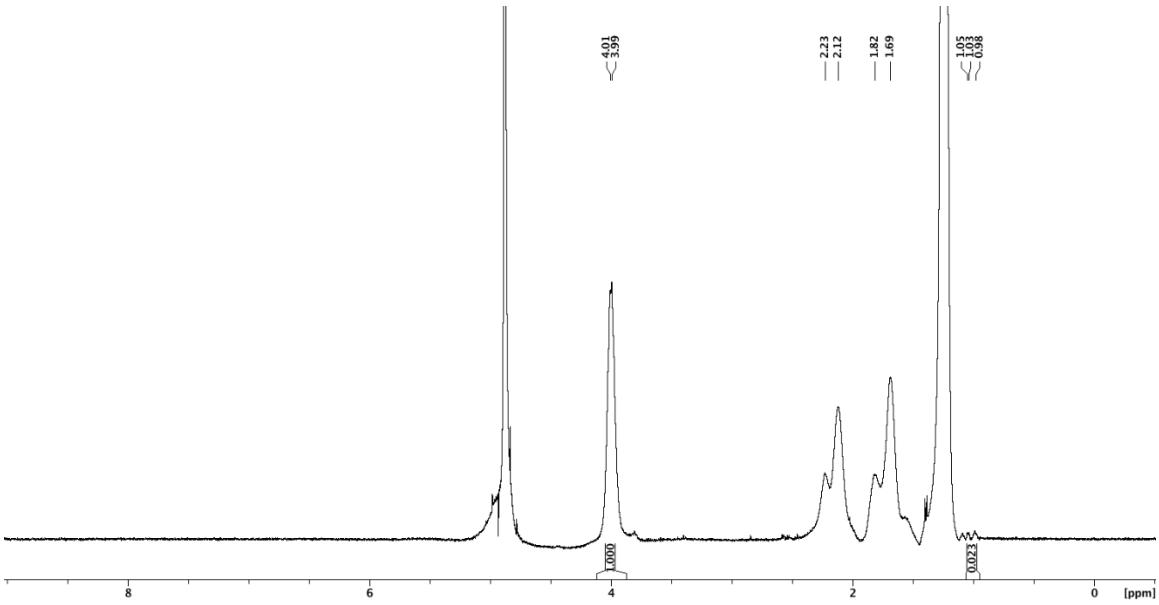

Figure 11. ^{1}H NMR spectrum of poly(NIPAAm-*co*-GAPGLL-NH_2).

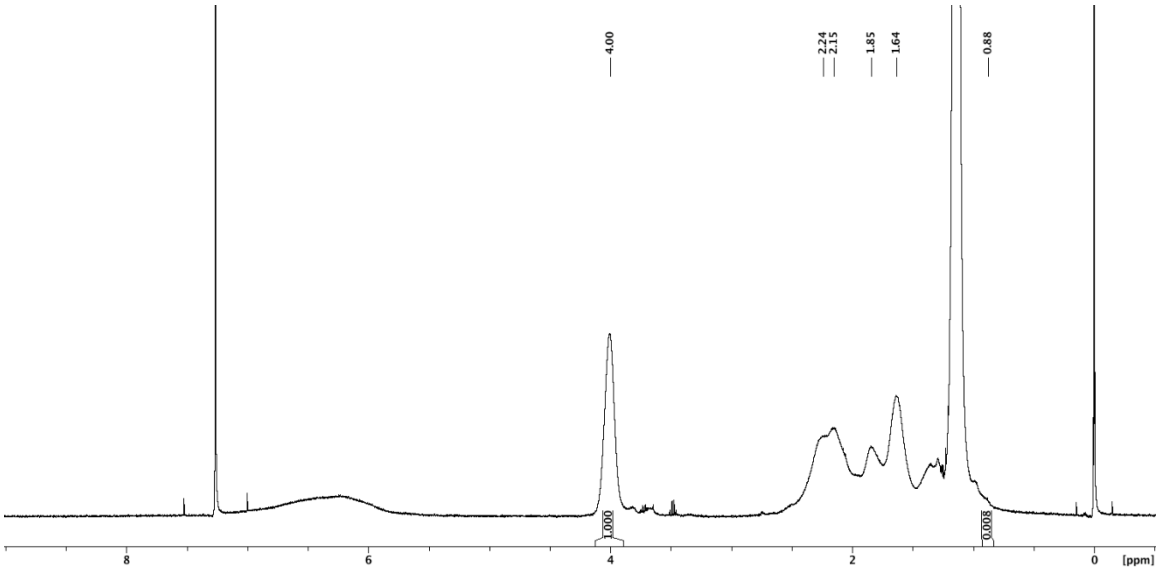

Figure 12. ^{1}H NMR spectrum of poly(NIPAAm-*co*-GAPGLV-NH_2) with 4 mol% peptide in feed.

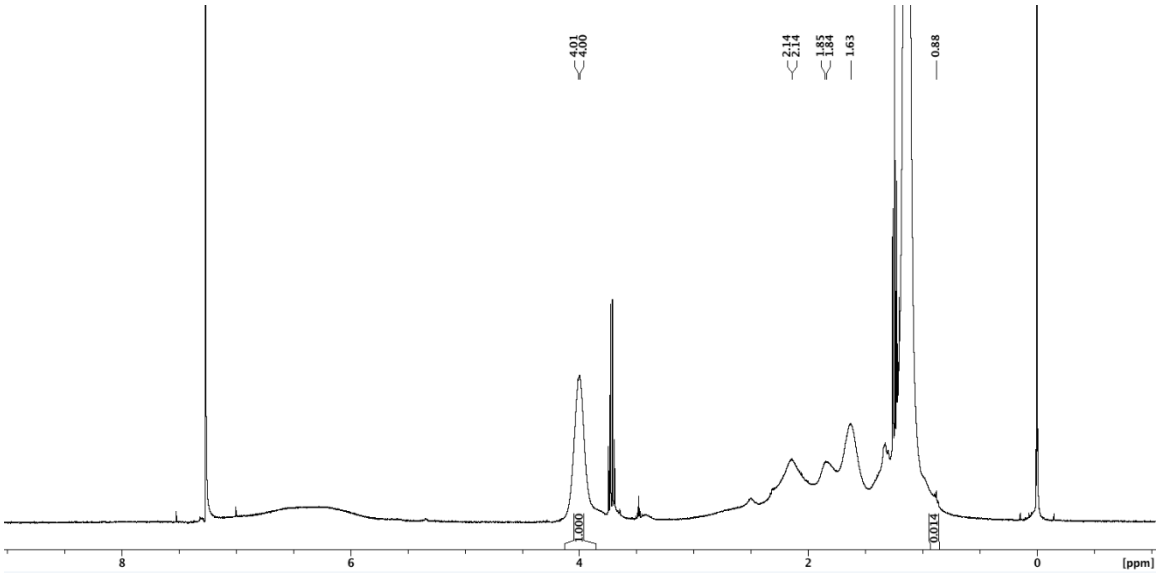

Figure 13. ^{1}H NMR spectrum of poly(NIPAAm-*co*-GAPGLV-NH_2) with 8 mol% peptide in feed.

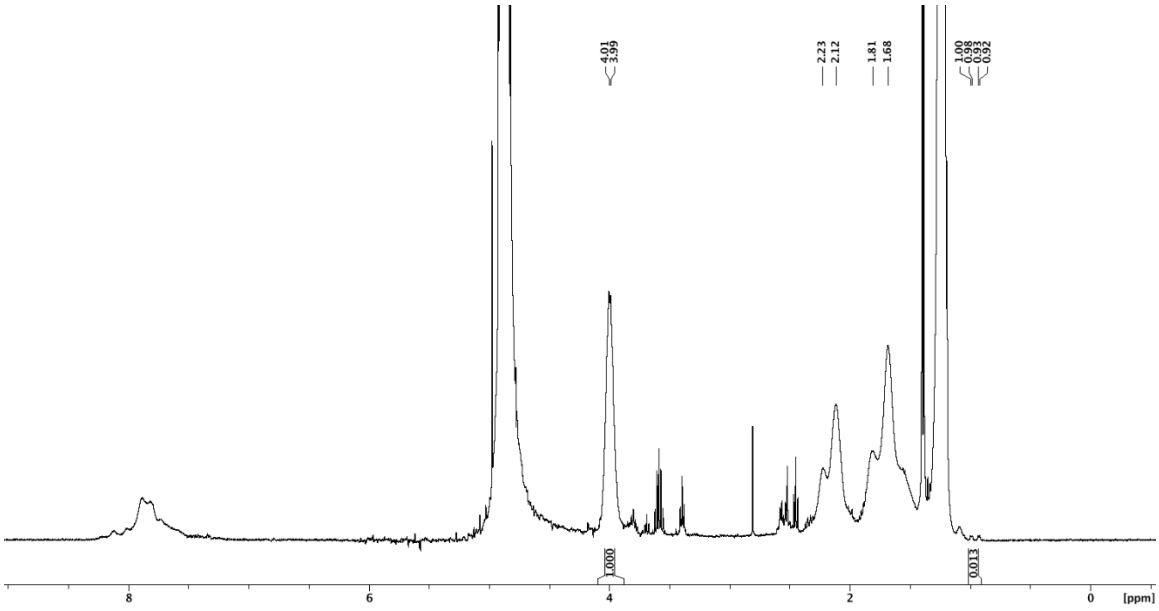

Figure 14. [1]H NMR spectrum of poly(NIPAAm-*co*-GAPGLF-COOH) with 2 mol% peptide in feed.

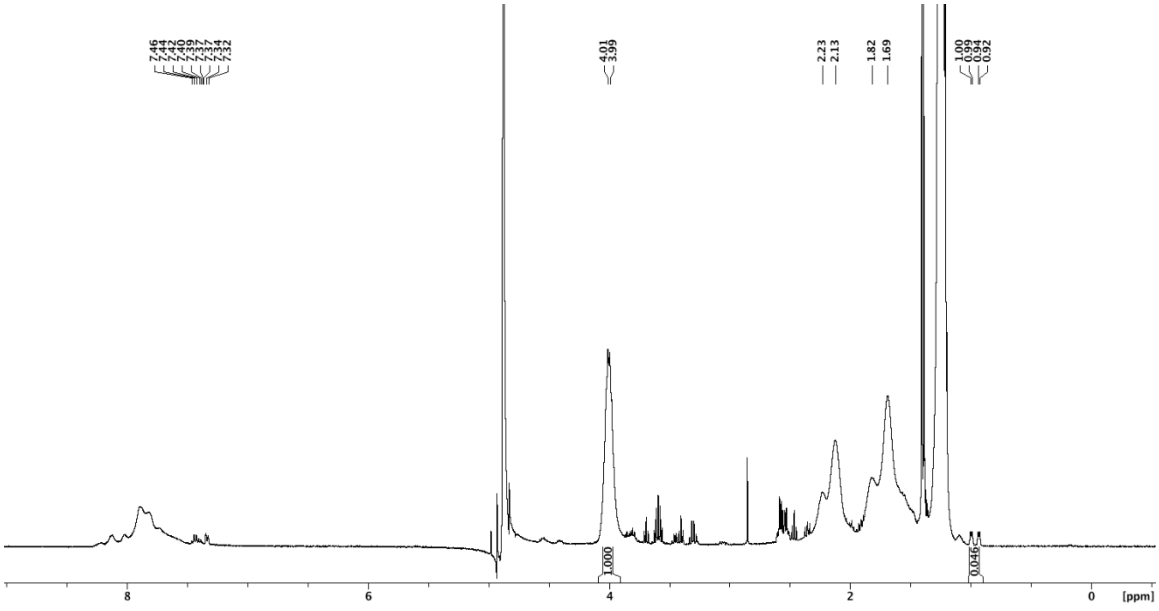

Figure 15. [1]H NMR spectrum of poly(NIPAAm-*co*-GAPGLF-COOH) with 8 mol% peptide in feed.